



OPEN ACCESS

EDITED BY

Venkata Vivek Reddy Palicharla,
University of Texas Southwestern Medical
Center, United States

REVIEWED BY

Swapnil Shinde,
Indian Institute of Technology Bombay, India
Rohit Sai Reddy Konada,
University of Texas Southwestern Medical
Center, United States

*CORRESPONDENCE

Uwe Wolfrum,
✉ wolfrum@uni-mainz.de

†PRESENT ADDRESSES

Deva Krupakar Kusuluri, Gena HealthX Private
Limited, Business Development Centre,
Heidelberg, Germany
Sarita Rani Patnaik, KAUST Smart-Health
Initiative and Biological and Environmental
Science and Engineering (BESE) Division, King
Abdullah University of Science and Technology
(KAUST), Jeddah, Saudi Arabia

†These authors have contributed equally to
this work

RECEIVED 31 October 2024

ACCEPTED 03 February 2025

PUBLISHED 04 March 2025

CITATION

Linnert J, Kusuluri DK, Güler BE, Patnaik SR,
May-Simera HL and Wolfrum U (2025) The BBS/
CCT chaperonin complex ensures the
localization of the adhesion G protein-coupled
receptor ADGRV1 to the base of primary cilia.
Front. Cell Dev. Biol. 13:1520723.
doi: 10.3389/fcell.2025.1520723

COPYRIGHT

© 2025 Linnert, Kusuluri, Güler, Patnaik, May-
Simera and Wolfrum. This is an open-access
article distributed under the terms of the
[Creative Commons Attribution License \(CC BY\)](https://creativecommons.org/licenses/by/4.0/).
The use, distribution or reproduction in other
forums is permitted, provided the original
author(s) and the copyright owner(s) are
credited and that the original publication in this
journal is cited, in accordance with accepted
academic practice. No use, distribution or
reproduction is permitted which does not
comply with these terms.

The BBS/CCT chaperonin complex ensures the localization of the adhesion G protein-coupled receptor ADGRV1 to the base of primary cilia

Joshua Linnert^{1†}, Deva Krupakar Kusuluri^{1†*}, Baran E. Güler¹,
Sarita Rani Patnaik^{2†}, Helen Louise May-Simera² and
Uwe Wolfrum^{1,3*}

¹Institute of Molecular Physiology, Molecular Cell Biology, Johannes Gutenberg University Mainz, Mainz, Germany, ²Institute of Molecular Physiology, Cilia Biology, Johannes Gutenberg University Mainz, Mainz, Germany, ³Institute for Quantitative and Computational Biosciences (IQCB), Johannes Gutenberg University Mainz, Mainz, Germany

Primary cilia are antenna-like sensory organelles present on almost all eukaryotic cells. Their sensory capacity relies on receptors, in particular G-protein-coupled receptors (GPCRs) which localize to the ciliary membrane. Here we show that ADGRV1, a member of the GPCR subfamily of adhesion GPCRs, is part of a large protein network, interacting with numerous proteins of a comprehensive ciliary proteome. ADGRV1 is localized to the base of prototypic primary cilia in cultured cells and the modified primary cilia of retinal photoreceptors, where it interacts with TRiC/CCT chaperonins and the Bardet Biedl syndrome (BBS) chaperonin-like proteins. Knockdown of ADGRV1, CCT2 and 3, and BBS6 result in common ciliogenesis phenotypes, namely reduced ciliated cells combined with shorter primary cilia. In addition, the localization of ADGRV1 to primary cilia depends on the activity of a co-complex of TRiC/CCT chaperonins and the BBS chaperonin-like proteins. In the absence of components of the TRiC/CCT-BBS chaperonin co-complex, ADGRV1 is depleted from the base of the primary cilium and degraded via the proteasome. Defects in the TRiC/CCT-BBS chaperonin may lead to an overload of proteasomal degradation processes and imbalanced proteostasis. Dysfunction or absence of ADGRV1 from primary cilia may underly the pathophysiology of human Usher syndrome type 2 and epilepsy caused by mutations in *ADGRV1*.

KEYWORDS

primary cilia, adhesion GPCR, t-complex protein ring complex (TRiC), chaperonin containing Tcp-1 (CCT), Chaperonin-like BBS proteins, proteasomal degradation, usher syndrome, epilepsy

Introduction

Primary cilia are antenna-like organelles that can protrude from the cell membrane of most animal cells and receive external signals from the cellular environment (Mill et al., 2023). The microtubule pairs of their characteristic axoneme project from the mother centriole of the basal body, across the transition zone and into the cilia shaft of the cilia membrane. For their sensory function, primary cilia are equipped with numerous

membrane receptors which convert the various external signals into intracellular signaling pathways (Satur and Christensen, 2007; Mill et al., 2023). Most of these receptors of primary cilia are G-protein-coupled receptors (GPCRs) localized to the ciliary membrane. Here, we focus on ADGRV1 in cilia, an adhesion G protein-coupled receptor (aGPCR) which is a subclass of G protein-coupled receptors (GPCRs). As seen in other aGPCRs, ADGRV1 features a unique combination of the GPCR characteristic seven-transmembrane helix domain (7TM) resembling the “receptor unit”, which transduces extracellular signals and mediates intracellular G-protein coupling via conformational changes, as well as an extracellular adhesion unit (Langenhan, 2020; Knapp et al., 2022). The extracellular N-terminal fragment (NTF) of aGPCRs can be released from the C-terminal fragment (CTF) by autoproteolytic cleavage at the GPCR proteolysis site in the GAIN (GPCR autoproteolysis-inducing) domain. This enables a tethered intramolecular agonist, the so-called “Stachel” sequence which comprises the first 5–10 amino acids of the CTF, to interact with the surface of the 7TM triggering the activation of aGPCRs (Scholz et al., 2019; Knapp et al., 2022; Liebscher et al., 2022). Interestingly, ADGRV1 can alternatively couple to two different heterotrimeric G-protein α -subunits (Shin et al., 2013; Hu et al., 2014) which may switch upon autoproteolytic cleavage and “Stachel”-mediated activation (Knapp et al., 2022).

Numerous mutations in the human *ADGRV1* gene are causative for the human Usher syndrome type 2 (USH2C) (Weston et al., 2004). The human Usher syndrome (USH) is the most common form of combined hereditary deaf-blindness, characterized by both clinical and genetic heterogeneity. Up to four USH subtypes are related to defects in at least 11 genes (Fuster-García et al., 2021). Over the years, evidence has accumulated that USH could be classified as a ciliopathy, since USH molecules are often associated with primary cilia (Liu et al., 1997; Reiners et al., 2006; Maerker et al., 2008; Sorusch et al., 2017; 2019; Mill et al., 2023). In addition, more recently, mutations in *ADGRV1* have been associated with various forms of epilepsy (Wang et al., 2015; Myers et al., 2018; Liu et al., 2020; Leng et al., 2022; Zhou et al., 2022). Interestingly, there is recent emerging evidence, though, that defects in cilia are linked to the development of epilepsy (Karalis et al., 2022; Limerick et al., 2024; Vien et al., 2023).

The defects that most likely underlie USH2C are found in the sensory cells of the two sensory organs affected by USH, the auditory hair cells of the inner ear and the photoreceptor cells of the retina. Adhesion fibres, which are formed by the long extracellular domain of ADGRV1 and connect neighbouring membranes, are lost in *Adgrv1*-deficient mouse models (McGee et al., 2006; Michalski et al., 2007; Maerker et al., 2008). However, almost nothing is known about the pathomechanisms that lead to epilepsy associated with mutations in *ADGRV1*.

ADGRV1, previously named as very large GPCR 1 (VLGR1) is one of the largest receptor proteins of the human body with up to ~6,300 amino acid residues and a molecular weight of ~700 kDa (McMillan et al., 2002; McMillan and White, 2010; Hamann et al., 2015). ADGRV1 is almost ubiquitously expressed in mammals, with particularly high expression in the nervous system and the sensory cells of the inner ear and the eye (Güler et al., 2024; McMillan and White, 2010; Uhlén et al., 2015; <https://www.proteinatlas.org/search/ADGRV1>). We and others previously showed that

ADGRV1 is part of various cellular adhesions: focal adhesions (Kusuluri et al., 2021; Güler et al., 2023), mitochondria-associated ER membranes (MAMs) (Krzysko et al., 2022), synapses between neurons, and neurons and glial cells (Reiners et al., 2005; Specht et al., 2009; Güler et al., 2024), ankle-links of developing hair cell stereocilia (McGee et al., 2006; Michalski et al., 2007) and the periciliary membrane complex at the base of the light-sensitive outer segment of vertebrate photoreceptor cells (Maerker et al., 2008).

Recent omics data and preliminary data on primary cilia in hTERT-immortalized retinal pigment epithelial cells (hTERT-RPE) indicated that ADGRV1 is a common molecular component of primary cilia (Knapp et al., 2022). We recently showed that ADGRV1 interacts not only with several other USH proteins but also with the CCT molecules of hetero-octameric TriC/CCT chaperonin complex and the three Bardet-Biedel syndrome (BBS) chaperonin-like proteins (BBS10, BBS12, and BBS6 also known as MKKS (McKusick-Kaufman-Syndrom) protein) in primary cilia (Linnert et al., 2023b) known to mediate the assembly of the BBSome at primary cilia (Seo et al., 2010; Zhang et al., 2012). However, whether ADGRV1 serves as a substrate of the TriC/CCT/BBS chaperone co-complex remained unsolved.

Here, we identify potential interaction partners of ADGRV1 in the ciliary proteome and show a genetic/transcriptional interaction of *ADGRV1* and several genes of the primary ciliary core. We reveal that the absence of ADGRV1 and components of the TriC/CCT/BBS chaperone co-complex leads to a common phenotype manifested in reduced ciliogenesis and ciliary length. Furthermore, we show that in the absence of the functional TriC/CCT/BBS chaperone co-complex, ADGRV1 is depleted from the ciliary base by proteasomal degradation. Dysfunction or absence of ADGRV1 from primary cilia may underlay the pathophysiology of human Usher syndrome type 2 and specific forms of epilepsy caused by mutations in *ADGRV1*.

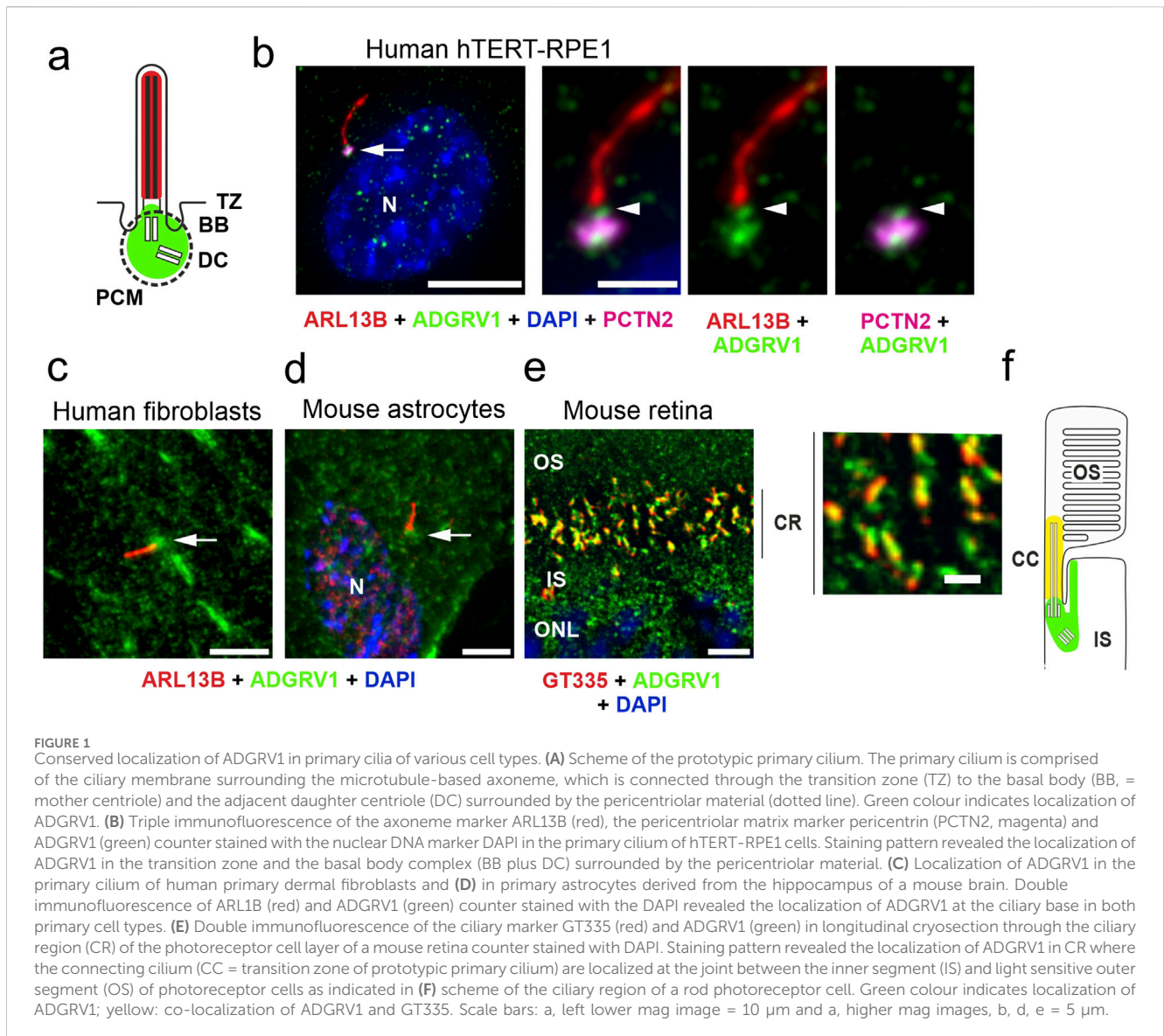
Results

Localization of ADGRV1 at the base of primary cilia

To explore the general ciliary localization of ADGRV1, we co-immunostained ADGRV1 with the primary ciliary markers, anti-ARL13B or anti-GT335 and the nuclear DNA marker DAPI in primary human dermal fibroblasts, murine primary brain astrocytes and the mouse retinal photoreceptor cells (Figure 1). We could show by immunofluorescence microscopy that ADGRV1 is localized to the base of primary cilia of human fibroblasts, mouse astrocytes, and retinal photoreceptor cells (Figure 1).

Analysis of tandem affinity purification data revealed interactions of ADGRV1 with core proteins of primary cilia

To determine potential molecular interactions of ciliary molecules with ADGRV1 we screened the existing datasets of mass spectrometry analyzed tandem affinity purifications (TAPs) with ADGRV1 constructs as baits (Figure 2A) (Knapp et al., 2022)



for proteins of the ciliary proteome. For this, we compiled the cilia proteome by combining CiliaCarta (Van Dam et al., 2019) and the SYSCILIA gold standard v2 (Vasquez et al., 2021) identifying 1,178 ciliary proteins (Supplementary Table S1). The comparison of this ciliary proteome with the hits of the ADGRV1 TAPs revealed 116 proteins as putative interaction partners of ADGRV1 associated with primary cilia (Supplementary Table S2). Most of the potentially interacting proteins were observed in the TAP datasets of the N- and C-terminally tagged CTFs (81 and 69, respectively) and ADGRV1a (70) with a high degree of overlap (Figure 2B). This indicates that ciliary proteins may preferentially interact with the 7TM domain of the receptor unit of ADGRV1. Subsequently, STRING analysis demonstrates that the identified potential interaction proteins are integrated into a large protein network (Figure 2C). The interaction of ADGRV1 with some of the potential interaction partners identified in the ciliary proteome by our systems biology approach has been experimentally confirmed via diverse interaction assays (Reiners et al., 2005; van Wijk et al., 2006; Zou

et al., 2017; Knapp et al., 2022; Linnert et al., 2023b). Among them are CCTs and the splicing factor PRPF6, in addition to other USH proteins, such as scaffold proteins USH1C/harmonin and WHRN/whirlin (USH2D).

Ciliary genes are differentially expressed in the transcriptomes of human USH2C patient-derived fibroblasts and the retina of *Adgrv1* deficient mice

We examined the effects of ADGRV1 deficiency on the expression of ciliary genes in cells and tissue previously obtained from dermal fibroblasts derived from a USH2C patient with the biallelic pathogenic variant *ADGRV1*^{Arg2959*} compared to a healthy individual (Güler et al., 2024), and of retinas derived from the *Adgrv1*/del7TM mouse model compared to wild type (wt) control mice (Linnert et al., 2023a). We screened these transcriptomes for

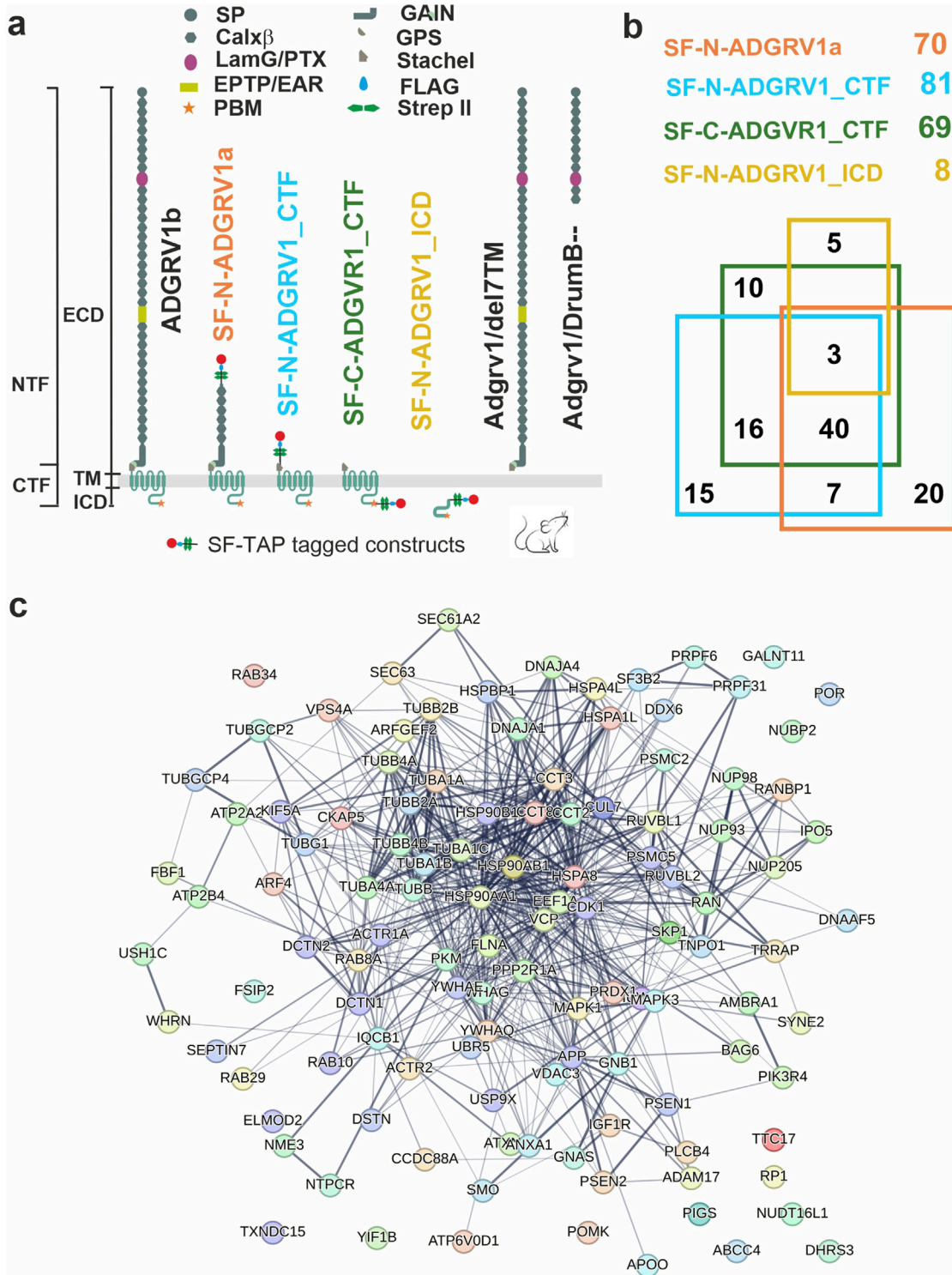


FIGURE 2 Interactions of ADGRV1 with proteins of primary cilium revealed by affinity proteomics. **(A)** Schematic representation of full length ADGRV1b, ADGRV1 bait constructs used in the tandem affinity purifications (Knapp et al., 2022), and truncated ADGRV1 proteins expressed in Adgrv1/del7TM and Adgrv1/DrumB-mouse models due to a deletion of the 7TM domain or a premature termination codon (McMillan and White, 2004; Potter et al., 2016). **(B)** Venn diagram of ADGRV1 prey assigned to the primary cilia proteome defined by the CiliaCarta and the Syscilia consortium (Van Dam et al., 2019; Vasquez et al., 2021). **(C)** The interaction of the prey, identified in b, visualised in a STRING network.

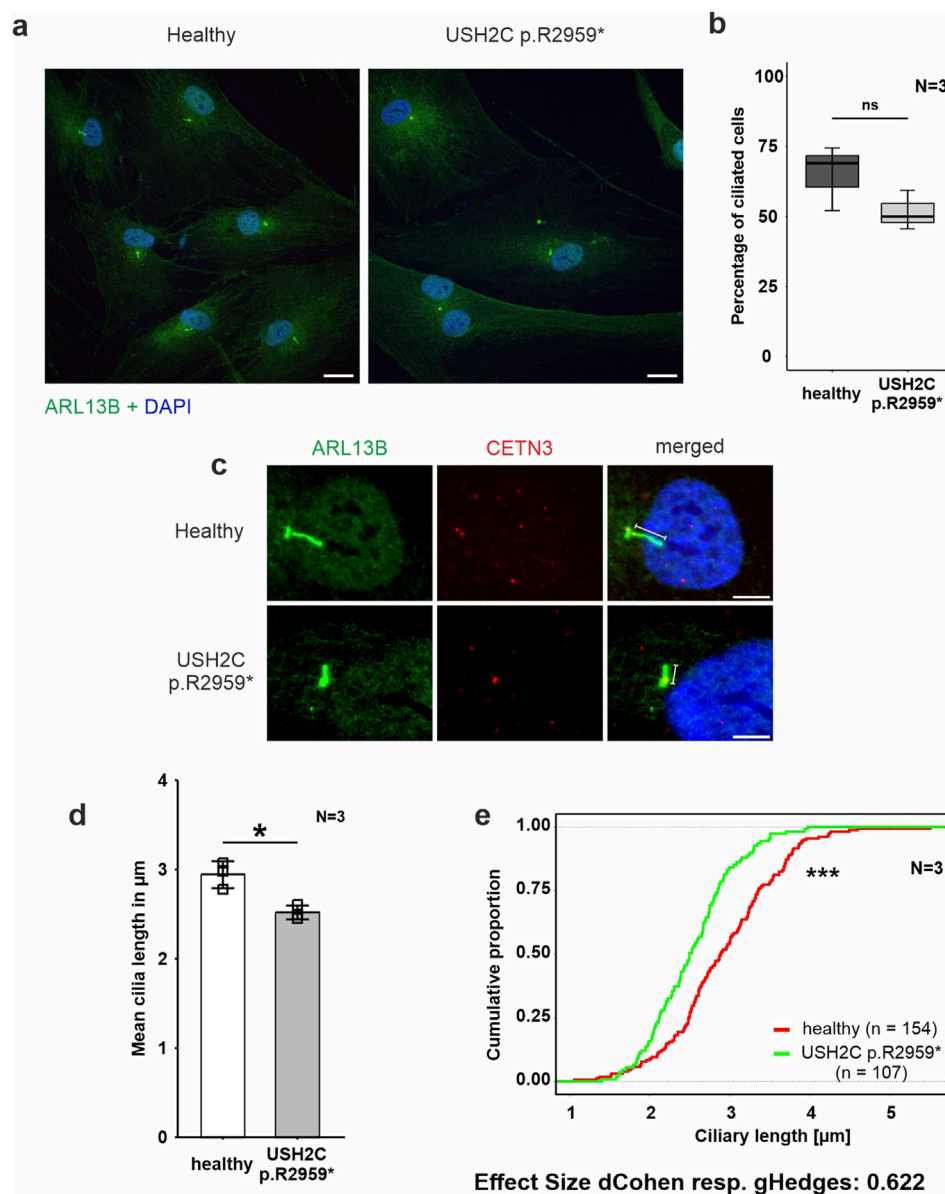


FIGURE 4

Phenotypic analysis of primary cilia of fibroblasts derived from a USH2C patient (A–E) Immunofluorescence double staining of the axonemal marker ARL13B (green) and the ciliary base marker centrin 3 (CENT3, red) counterstained with nuclear DNA marker DAPI (blue) in patient-derived USH2C p. R2959* fibroblasts and healthy control cells. (B, D, E) Quantitative analysis of the number of ciliated cells, the mean cilia length and the distribution of cilia length in patient-derived fibroblasts and healthy control cells. Quantification revealed no significant changes in the number of ciliated cells, but significantly shorter cilia in the patient-derived fibroblasts compared to the healthy controls. N = number of biological replicates, n = number of analysed cells. Statistical significance was determined by the two-tailed Student's t-test (B, D) and the Kolmogorov-Smirnov test (E): * $p < 0.05$, ** $p < 0.01$, *** $p < 0.005$. Scale bar in a = 20 μm , c = 5 μm .

ciliary genes present in the combined datasets of CiliaCarta (Van Dam et al., 2019) and the SYSCILIA gold standard v2 (Vasquez et al., 2021) (Supplementary Table S1).

We identified 39 differentially expressed genes (DEGs) (17 upregulated and 22 downregulated), in USH2C patient-derived fibroblasts (Figure 3A). By applying STRING analysis, we found that the proteins corresponding to these genes organize in several distinct subclusters (Figure 3B). Gene Ontology (GO) term analysis revealed that these ciliary DEGs were associated with the two *biological process* subcategories *G protein-coupled receptor*

signaling pathway and *signaling* (Figure 3C; Supplementary Table S3).

In the retina of *Adgrv1/del7TM* mice, 70 ciliary genes were differentially expressed (49 upregulated and 21 downregulated) (Figure 3D). STRING analysis revealed the proteins encoded by these ciliary DEGs into a protein-protein interaction network composed of two linked clusters (Figure 3E). Further analysis of these protein clusters showed their association with phototransduction and supporting proteins such as chaperones or vesicular transport proteins, respectively. GO term enrichment

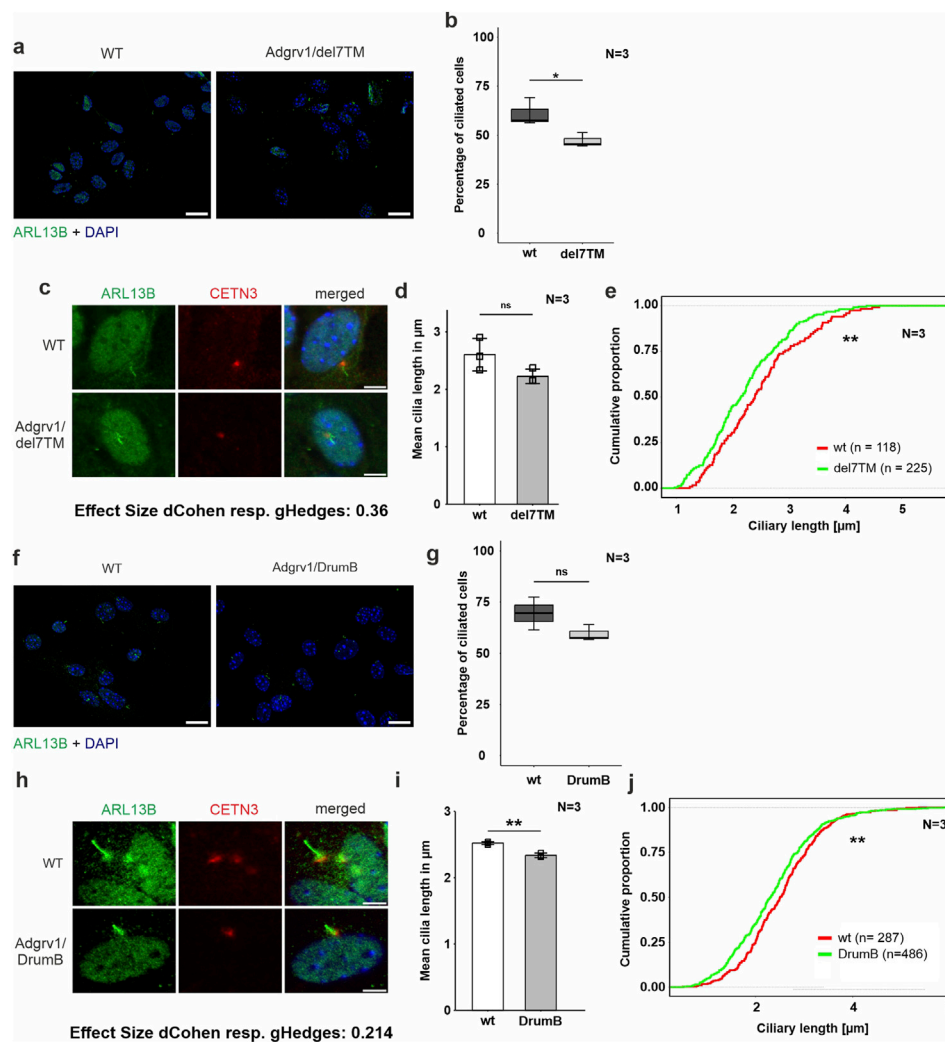


FIGURE 5

Phenotypic analysis of primary cilia of primary astrocytes isolated from brains of *Adgrv1*-deficient mouse models (A, C) Immunofluorescence double staining of the axonemal marker ARL13B (green) and the ciliary base marker centrin 3 (CETN3, red) counterstained with nuclear DNA marker DAPI (blue) in primary astrocytes derived from *Adgrv1/del7TM* mice and wt controls. In (A) an overview of the ciliated cells is demonstrated and in (C) a magnification of the primary cilia is shown. (B, D, E) Quantitative analysis of the number of ciliated cells (B), the mean cilia length (D) and the distribution of cilia length (E) of primary astrocytes revealed a significant decrease of ciliated cells in *Adgrv1/del7TM* astrocytes, no significantly altered mean cilia length, but a significant reduction of the cilia length quantifying the overall cilia length distribution. (F, H) Immunofluorescence double staining of the axonemal marker ARL13B (green) and the ciliary base marker centrin 3 (CETN3, red) counterstained with nuclear DNA marker DAPI (blue) in primary astrocytes derived from *Adgrv1/DrumB* mice and wt controls. Overview of ciliated cells (F), and magnification of primary cilia (H). Quantitative analysis of the number of ciliated cells (G), the mean cilia length (I) and the distribution of cilia length (J) of primary astrocytes revealed no significant decrease of ciliated cells in *Adgrv1/DrumB* astrocytes, but a significant reduction in the mean cilia length and the cilia length distribution. N = number of biological replicates, n = number of analysed cells. Statistical significance was determined by the two-tailed Student's t-test (B, D, G, I) and the Kolmogorov-Smirnov test (E, J): * $p < 0.05$, ** $p < 0.01$, *** $p < 0.005$. Scale bars: a, e, i = 5 μm .

analysis revealed common links between the DEGs. In the category *cellular component*, we found 19 genes related to the term 9 + 0 non-motile cilium and 20 genes of the broader term *non-motile cilium*. Additionally, several genes were allocated to GO terms related to retinal photoreceptor cells, namely 14 genes to *photoreceptor outer segment*, 18 genes to *photoreceptor cell cilium* and 13 genes to *visual perception* (Figures 3F, G; Supplementary Table S4).

In summary, the absence of *ADGRV1* resulted in dysregulation of the expression of genes associated with primary cilia and the highly specialized primary cilium of retinal photoreceptor cells. Defects in several of these ciliary DEGs have been associated with USH (*Cep250* (atypical USH) (Khateb et al., 2014), *Pcdh15*

(USH1F) (Ahmed et al., 2001) or other retinal ciliopathies *Fam164a* (RP28) (Bandah-Rozenfeld et al., 2010; Langmann et al., 2010; Karlstetter et al., 2014) leading to retinal degenerations as seen in USH2C patients with pathogenic variants in the *ADGRV1* gene.

Ciliation and ciliary length is affected in human and murine primary cell models deficient for ADGRV1

We studied primary cilia in the following cellular models: human USH2C *ADGRV1*^{Arg2959*} patient dermal fibroblasts

(Figure 4) and mouse primary brain astrocytes derived from *Adgrv1/del7TM* and *Adgrv1/DrumB* mice (Figure 2A) in comparison to appropriate controls (Figure 5).

Fibroblasts were starved for 48 h in serum-free media to induce ciliation prior to immunohistochemical staining for the ciliary axoneme marker ARL13B and the ciliary base marker centrin 3 (Figure 4A). Fluorescence microscopy revealed reduced numbers of ciliated USH2C patient fibroblasts compared to healthy controls (Figure 4B). To determine the ciliary length, we measured the length of the ARL13B positive axoneme projecting from the centrin 3 positive ciliary base, calculated the mean of ciliary length (Figure 4C), and plotted the distribution of ciliary length (Figures 4C, D). Statistical evaluation of both analyses revealed a significant decrease in length in USH2C patient fibroblasts compared to healthy controls.

To analyze ciliogenesis in primary astrocytes we isolated astrocytes from the hippocampi of *Adgrv1/del7TM*, *Adgrv1/DrumB*, and wt control mice following our previously established protocol (Güler et al., 2021). Astrocytes were starved for 48 h in serum-free media and stained for ciliary markers ARL13B and centrin 3 prior to fluorescence microscopic analysis (Figure 5). Fluorescence microscopy revealed reduced numbers of ciliated astrocytes derived from both the *Adgrv1/del7TM* and *Adgrv1/DrumB* mice compared to wt controls (Figures 5A, E). However, due to the high variability in the three independent experiments, statistical test revealed significantly reduced numbers of ciliated astrocytes only for *Adgrv1/del7TM* cells (Figures 5B, F).

Ciliary length measurements revealed shorter primary cilia of primary astrocytes isolated from both *Adgrv1*-deficient mouse models (Figures 5C, D, G, H). While in primary astrocytes of *Adgrv1/DrumB* mice both, the mean length and the length distribution of primary cilia were significantly different (Figures 5G, H) only the length distribution of primary cilia from *Adgrv1/del7TM* was significantly different (Figures 5C, D) compared to control.

Overall, we observed ciliary phenotypes in all ADGRV1-deficient cells tested, which manifested in the reduced number of ciliated cells and in a reduced length of primary cilia.

Reduced length of the connecting cilium in photoreceptor cells of the *Adgrv1/del7TM* mouse retina

The light-sensitive outer segments of the photoreceptor cells of the vertebrate retina are highly modified primary sensory cilia characterized by an extended transition zone, named connecting cilium (Figure 1) (Roepman and Wolfrum, 2007; May-Simera et al., 2017). To determine whether the absence of ADGRV1 in photoreceptor cilia is also associated with a ciliary phenotype, we determined the length of the connecting cilium in the *Adgrv1/del7TM* mouse retina compared to wild-type mice. We immunostained the connecting cilium of photoreceptors in longitudinal retinal cryosections with antibodies against centrin 3 and GT335, both previously demonstrated as robust markers for the connecting cilium (Figures 6A, B) (Wolfrum, 1995; Grotz et al., 2022). Quantification of the mean cilia length and distribution revealed a significant reduction of connecting cilia length in the

retinal photoreceptor cells of *Adgrv1/del7TM* mice when compared to those of wt mice (Figures 6C, D). This confirms the phenotype of reduced cilia length in *Adgrv1*-deficient photoreceptor cells observed in primary cell models, namely, in dermal fibroblasts and brain astrocytes derived from USH1C patients and *Adgrv1* mouse models.

The absence of TriC/CCT-BBS chaperonin complex components reduces ciliary localization of ADGRV1

We have previously shown that ADGRV1 physically interacts with components of the TRiC/CCT chaperonin complex and the chaperonin-like BBS molecules (Linnert et al., 2023b). Here we tested whether the localization of ADGRV1 at primary cilia depends on the TRiC/CCT-BBS chaperone complex, by depletion of chaperone complex components and immunostaining for ADGRV1 (Figure 7).

For this, we depleted BBS6, CCT2, and CCT3 by siRNAs in hTERT-RPE1 cells (validation: Supplementary Figure S1), induced ciliogenesis by serum starvation and immunostained for ADGRV1 and the ciliary marker ARL13B (Figure 7). Fluorescence microscopy revealed that siRNA-mediated knockdowns of BBS6, CCT2, and CCT3 resulted in significant reductions of the intensity of the ADGRV1 immunofluorescence at the base of the primary cilium when compared to cells treated with non-targeting control (NTC) siRNAs (Figures 7A–D).

We also observed that the cilia length of the primary cilia was reduced after elimination of the three components of the TRiC/CCT/BBS chaperonin complex (Supplementary Figures S2A–D). Interestingly, the knockdown of BBS6 did not alter the localization of CCT3 at the base of the cilium compared to that of the control cells (Supplementary Figure S3).

Next, we investigated whether the absence of BBS chaperonins also affects the distribution of ADGRV1 in the photoreceptor cilia (Figure 7E). For this, we immunostained *Adgrv1* in the retinae of *Bbs6^{-/-}* and *Bbs10^{-/-}* knockout mice and a wt control. Fluorescence microscopy of immunostained retinal longitudinal cryosections revealed prominent localization of *Adgrv1* at the connecting cilium of photoreceptor cells of control wt retinae as revealed by counterstaining for the connecting cilium marker centrin 2 (Wolfrum, 1995; Giessel et al., 2004), coherent with previous findings (van Wijk et al., 2006; Liu et al., 2007; Maerker et al., 2008; Yang et al., 2010). In comparison, localization of *Adgrv1* was reduced in the connecting cilia of photoreceptor cells in the *Bbs6^{-/-}* and *Bbs10^{-/-}* retinae (Figure 7E).

Together, these findings indicate that the ciliary localization of ADGRV1 depends on the TriC/CCT-BBS chaperones.

Depletion of BBS6 in hTERT-RPE1 cells leads to increased mRNA levels but decreased ADGRV1 protein expression

To validate whether the depletion of chaperonins affects the expression of *ADGRV1* we quantified the mRNA expression of

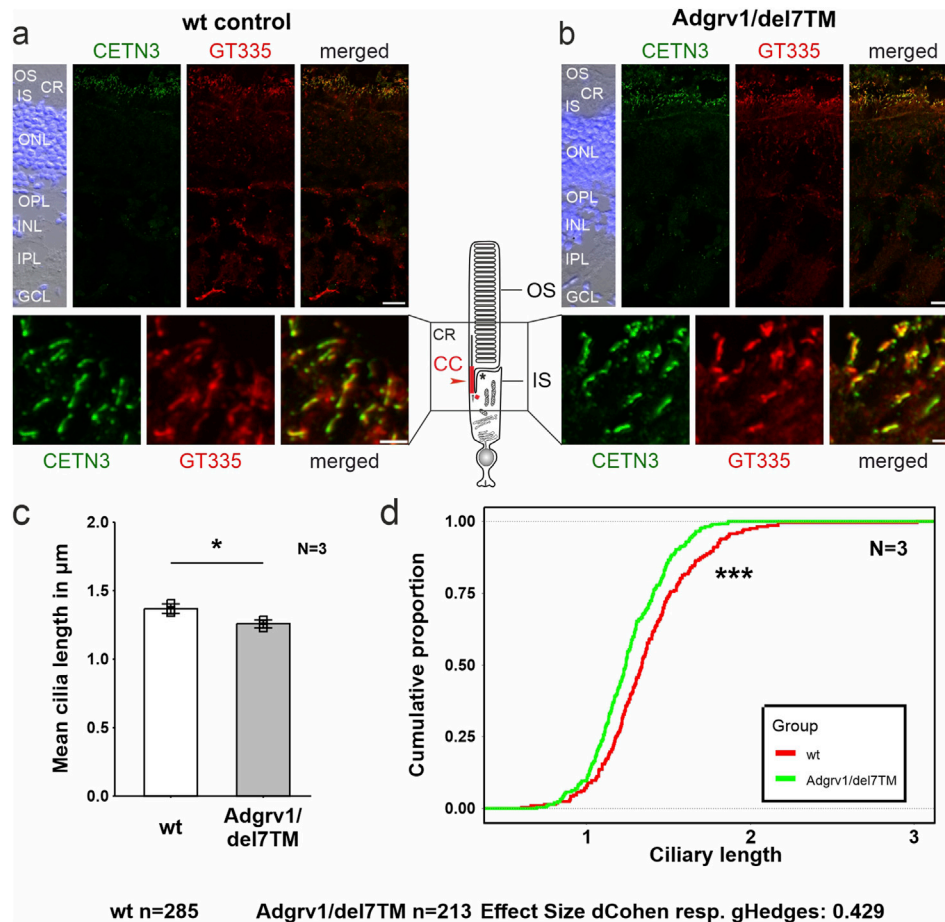


FIGURE 6

Primary cilium length in *Adgrv1/del7TM* retinas is reduced compared to wt controls. (A, B) Double immunofluorescence staining for centrin 3 (CETN3, green) and glutamylated tubulin (GT335) counterstained with DAPI in longitudinal cryosections through retinas of wt (A) and *Adgrv1/del7TM* mice (B). (C) Quantification of mean cilium length revealed a reduction in *Adgrv1/del7TM* retinas compared to wt controls confirmed by (D) the quantification of the distribution of the connecting cilium lengths. N = number of biological replicates, n = number of measured connecting cilia. Statistical significance was determined by the two-tailed Student's t-test (C) and the Kolmogorov-Smirnov test (D): *p < 0.05, **p < 0.01, ***p < 0.005. Scale bars: a, b = 15 μm and 2 μm .

ADGRV1 upon BBS6 knockdown in hTERT-RPE1 cells (Figure 7). Quantitative real-time PCR (qPCR) analysis revealed a significantly elevated expression of *ADGRV1* after siRNA-mediated knockdown of BBS6, while the expression of *CCT3* was not altered (Figures 8A, B). Next, we analyzed the mRNA expression of *Adgrv1* in the retina of *Bbs6*^{-/-} knockout mice. qPCR revealed that the expression of *Adgrv1* was significantly increased in postnatal 21 (P21) and P29 *Bbs6*^{-/-} mouse retinas compared to wt littermates (Figures 8C, D), confirming the upregulation of the expression of *Adgrv1* mRNA transcripts in tissue.

To test whether the expression of the translated *ADGRV1* protein is also affected by the depletion of BBS6 we performed Western blot analyses of lysates obtained from hTERT-RPE1 cells treated with siRNAs specific for BBS6 or NTC siRNA, respectively. Western blots probed with either antibodies against *ADGRV1* or *CCT3* revealed significantly reduced *ADGRV1* protein expression, but no changes in the *CCT3* protein expression in BBS6 knockdown cells (Figures 8E, F).

Taken together, in the absence of the BBS6 chaperonin *ADGRV1* mRNA expression is upregulated while in contrast *ADGRV1* protein levels are reduced. This suggests *ADGRV1* expression is additionally post-translationally controlled or compensated at the protein level.

Depletion of CCT/BBS chaperonins increases the proteasomal degradation of *ADGRV1*

To investigate whether the reduced *ADGRV1* protein expression observed in the absence of chaperonins is due to proteasomal degradation, we experimentally inhibited the proteasomal pathway by MG132. For this, we treated BBS6 knockdown hTERT-RPE1 cells after ciliogenesis induction with MG132. Quantification of Western blots showed that MG132 treatments compensated the significant decrease of *ADGRV1* protein expression following

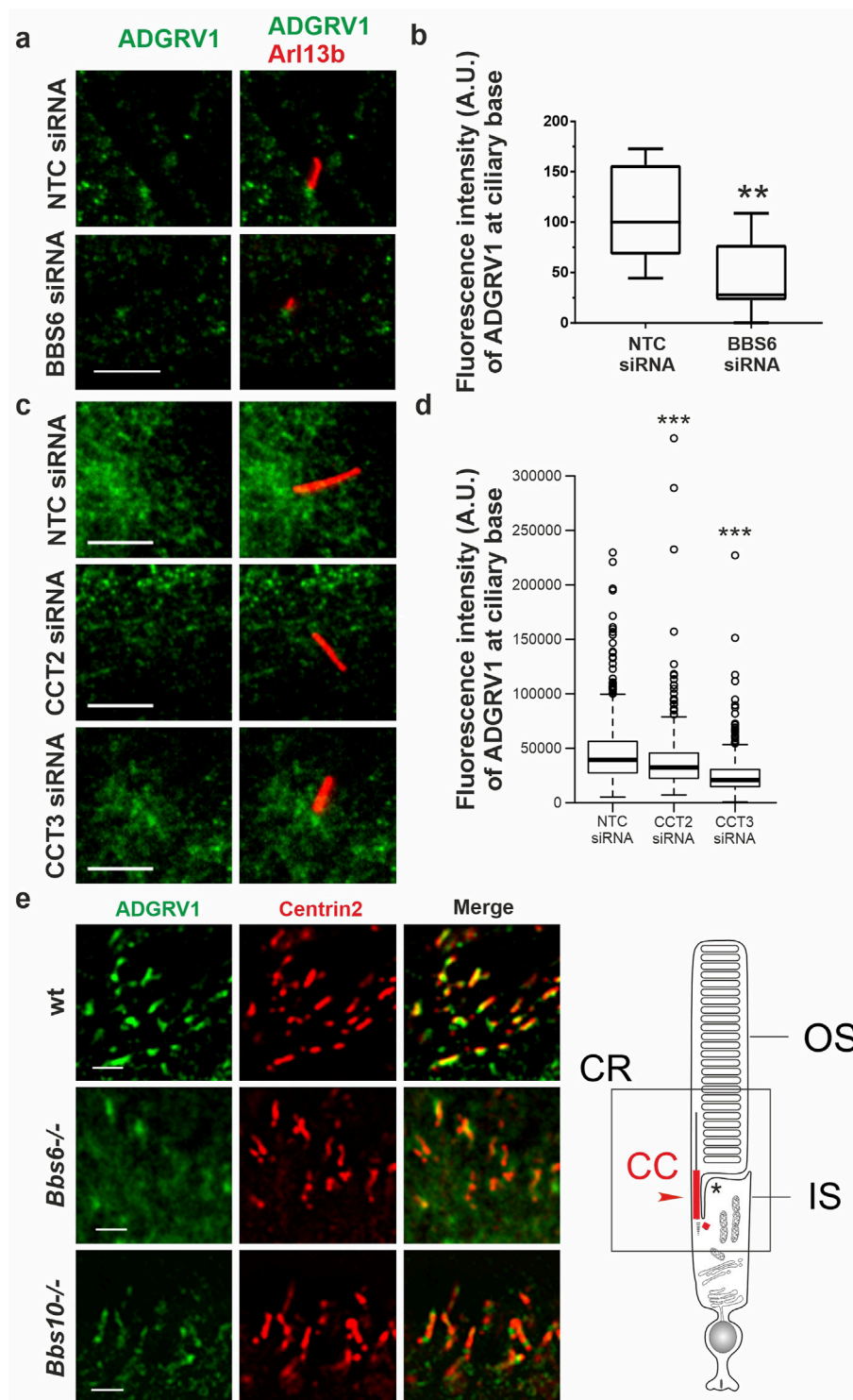


FIGURE 7

Immunofluorescence analysis of ADGRV1 in Tric/CCT-BBS chaperonin depleted cells and mouse retinæ (A, C) Double immunofluorescence staining for Arl13B (red) and ADGRV1 (green) of primary cilia in hTERT-RPE1 cells after siRNA-mediated knock down of (A) BBS6 and (B) CCT2 and CCT3 compared to non-targeting controls (NTC). (B, D) Quantification confirms reduced localization of ADGRV1 at the ciliary base upon BBS6 KD. (D) Quantification confirms reduced localization of ADGRV1 at the ciliary base upon CCT2 and CCT3 KD. (E) Double immunofluorescence staining for Adgrv1 (green) and connecting cilia marker Centrin2 (red) in longitudinal cryosections through the ciliary region (CR, in scheme left) of mouse photoreceptor cells revealed reduced Adgrv1 immunofluorescence in *Bbs6*^{-/-} and *Bbs10*^{-/-} mice when compared to wt littermate controls. Scheme shows CC: connecting cilium, OS: outer segment, IS: inner segment of a rod photoreceptor cell. Statistical significance was determined by the two-tailed Student's t-test: **p* < 0.05, ***p* < 0.01, ****p* < 0.005. Scale bars: a, c = 5 μm; e = 1 μm.

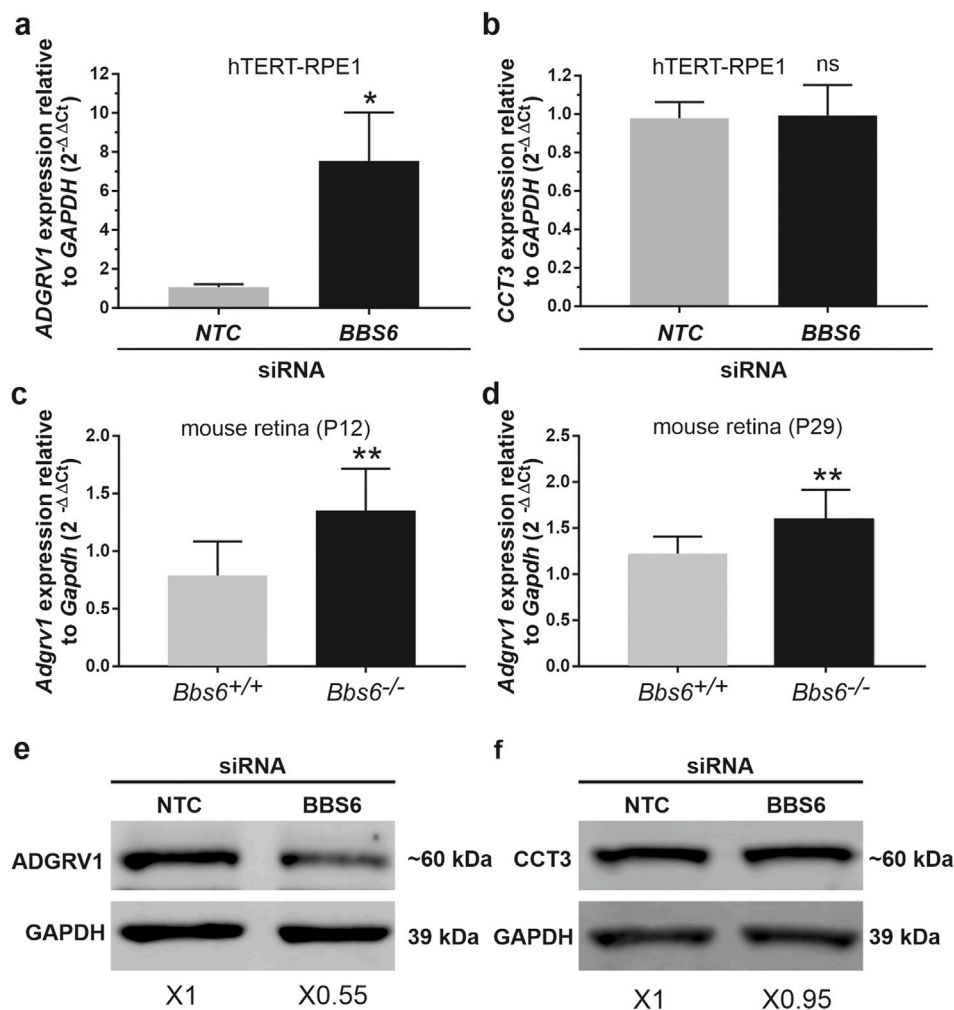


FIGURE 8

ADGRV1 mRNA and ADGRV1 protein expression are changed in the opposite direction in cells and tissues deficient for BBS6 (A) Quantitative real-time PCR (qRT-PCR) analysis of *ADGRV1* mRNA expression in serum-starved hTERT-RPE1 cells after siRNA-mediated *BBS6* knockdown compared to non-targeting control (NTC). (B) qRT-PCR analysis of *CCT3* mRNA expression in serum-starved hTERT-RPE1 cells after siRNA-mediated *BBS6* knockdown compared to non-targeting control (NTC). Quantifications revealed an increase of *ADGRV1* but not of *CCT3* mRNA expression in *BBS6* depleted cells. (C, D) qRT-PCR analysis of *Adgrv1* mRNA expression in retinæ of postnatal P12 and P29 *Bbs6*^{-/-} mice demonstrate significantly higher expression of *Adgrv1* mRNA. (E, F) Western blot analysis of ADGRV1 and CCT3 protein expression in serum-starved hTERT-RPE1 cells after siRNA-mediated *BBS6* knockdown. Quantifications of band densities revealed a decrease of ADGRV1 (x 0.55) but not of CCT3 expression (x 0.95) in *BBS6* depleted cells when compared to non-targeting controls (NTC). *GAPDH/Gapdh* and GAPDH protein were used as housekeeping control. Statistical significance was determined by the two-tailed Student's t-test: *p < 0.05, **p < 0.01, ***p < 0.005.

siRNA-mediated *BBS6* knockdown (Figures 9A, B) indicating ADGRV1 is degraded via the proteasome in the absence of the *BBS6* chaperonin.

Next, we validated these findings *in situ* by immunocytochemistry (Figures 9C, D). For this we co-stained primary cilia of hTERT-RPE1 cells for the ciliary axoneme marker ARL13B, ciliary base marker pericentrin-2 (PCNT2), and ADGRV1. Fluorescent microscopy revealed the depletion of the anti-ADGRV1 fluorescence between the ciliary base stained by anti-PCNT2 and the axoneme stained by anti-ARL13B which represents the transition zone after *BBS6* knockdown (Figures 9C, D). Quantification of ADGRV1 immunofluorescence confirmed that ADGRV1 protein remained in region of the ciliary transition zone when *BBS6* knockdown cells were treated with the MG132.

Together, this shows that ADGRV1 is prone to elevated proteasomal degradation in the absence of chaperonins.

Discussion

Primary cilia are antenna-like cellular protrusions serving as receiver hubs coordinating various incoming environmental signals (Mill et al., 2023). These signals are sensed and transduced via GPCRs for subsequent transmission via downstream intracellular G protein-mediated signaling pathways (Hilgendorf et al., 2024). In the present study, we focus on the adhesion GPCR ADGRV1, its localization to the primary cilia and its role in ciliogenesis.

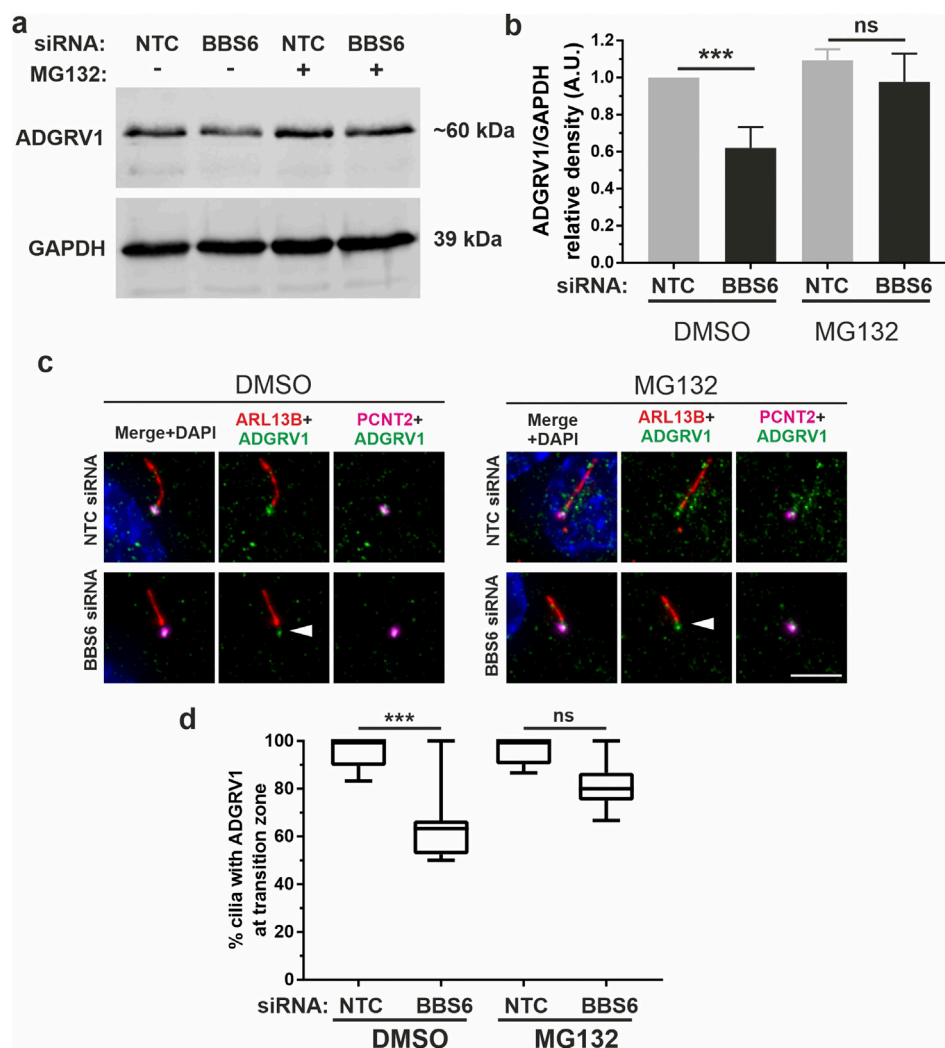


FIGURE 9
Increased proteasomal degradation of ADGRV1 upon BBS6 loss in hTERT-RPE1 cells. **(A, B)** Western blot analysis of ADGRV1 and CCT3 protein expression in serum-starved hTERT-RPE1 cells after siRNA-mediated *BBS6* knockdown treated with the proteasomal inhibitor MG132 solved in DMSO. The significant decrease of ADGRV1 protein expression in BBS depleted cells is restored by treatment with MG132. **(C, D)** Indirect immunofluorescence triple labelling of ADGRV1 (green) counterstained with axoneme marker ARL13B (red) and basal body marker pericentrin (PCNT2) (magenta) in NTC control and siRNA-mediated *BBS6* knockdown serum-starved hTERT-RPE1 cells treated with MG132 and DMSO. The ADGRV1 immunofluorescence in the transition zone of primary cilia (white arrowhead) is restored in cells treated with MG132. **(D)** Quantification of anti-ADGRV1 immunofluorescence intensity in the transition zone confirms recovery of ADGRV1 at the ciliary base and transition zone of *BBS6* KD cells upon MG132 treatment. Statistical significance was determined by the two-tailed Student's *t*-test: **p* < 0.05, ***p* < 0.01, ****p* < 0.005. Scale = 5 μ m.

We identified several potential interacting proteins of the ADGRV1 interactome from TAP datasets within the comprehensive ciliary proteome, which we compiled from previously published datasets (Van Dam et al., 2019; Vasquez et al., 2021). In addition, our analysis of the differential transcriptomes of ADGRV1 deficient cells and tissues points towards diverse roles of ADGRV1 in cilia-related pathways and ciliary function. Overall, the combined analyses of proteomic and transcriptomic data indicate that ADGRV1 functions as a receptor involved in primary cilia signaling. During GPCR signal transduction cascades, ligand-induced conformational changes in activated GPCRs can couple to several different G α subunits of heterotrimeric G proteins inducing different downstream signal pathways. Two alternative G α subunits Gai and Gas have been

previously described for ADGRV1 (Shin et al., 2013; Hu et al., 2014). More recently, we described that the activation of ADGRV1 by its autoproteolytic cleavage initiates the switch of G protein coupling from Gai to Gas (Knapp et al., 2022). Both α -subunits Gai to Gas have previously been described as GPCR signalling components in primary cilia (Hilgendorf et al., 2016). Accordingly, ADGRV1 can exert its dual function in primary cilia, firstly in adhesion, as found in the periciliary membrane complex of primary photoreceptor cilia (Maerker et al., 2008), and secondly in GPCR signal transduction and signaling coupled to G protein-mediated pathways. This hypothesis is supported by the differential transcriptomes obtained from the ADGRV1 deficient human USH2C patient fibroblast and the retina of the *Adgrv1/delta7TM* mouse model. GO term analysis of these differentially expressed genes

demonstrated that the expression of 44 genes assigned to the term “G protein coupled receptor signaling pathway” is altered in the absence of ADGRV1.

However, there is evidence that ADGRV1 is also related to other non-GPCR signaling pathways such as Wnt-, sonic hedgehog (Shh)- and Notch-pathway (Knapp et al., 2022). Here, we found that the expression of genes coding for key components of these signaling pathways such as the Gli2 or Wnt ligands are dysregulated in the absence of ADGRV1. While these data suggest a potential involvement of ADGRV1 in Wnt, Shh, and Notch signaling, it is important to note that these findings are based primarily on dysregulated gene expression rather than direct mechanistic evidence. Future studies should focus on elucidating the precise molecular mechanisms linking ADGRV1 to these signaling pathways. Nevertheless, all these pathways have in common that they play important, vital roles in regulating primary cilia function and maintenance (Mill et al., 2023; Hilgendorf et al., 2024). The disruption of GPCR and non-GPCR mediated ciliary signaling pathways can lead to ciliary phenotypes such as impaired ciliogenesis and altered cilia length (Avasthi and Marshall, 2012; Canterini et al., 2017; Lee, 2020; Mukherjee et al., 2020). As observed in defective ciliary signalling pathways, mutations and deficiencies in ADGRV1 also lead to a reduced number of ciliated cells and shorter cilia which is in line with ADGRV1's participation in signaling pathways of primary cilia.

A link between the DEGs identified in ADGRV1-deficient cells and tissues and the phenotype of shorter primary cilia can be found in the following two examples: *Kif5b* is significantly upregulated in *Adgrv1/del7TM* retinæ. The encoded kinesin protein controls the subcellular localization of the BBS-associated protein CCDC28B, which positively regulates cilia length (Novas et al., 2018). Overexpression of *Kif5b* reduces the amount of CCDC28B, which in turn leads to shorter cilia, as we found in *Adgrv1*-deficient retinæ. Cilia length is also controlled by NIMA-related kinase 10 (NEK10). NEK10 deficiency has been shown to reduce cilia length (Chivukula et al., 2020). Here, we found that *NEK10* expression is reduced in *USH2C* fibroblasts, which in turn correlates with shorter primary cilia. ADGRV1 is localized to the base of primary cilia, namely to the transition zone and the periciliary lattice surrounding the basal body (present study, Knapp et al., 2022). In photoreceptor cilia, ADGRV1 is additionally found together with other USH proteins in the periciliary membranes (Maerker et al., 2008). There, it is long extracellular domains form fibers that extend through the ciliary pocket and connect the cilia membrane of the transition zone to the periciliary plasma membrane. Overall, the ciliary base is a strategic compartment of the primary cilium that coordinates many essential ciliary functions. The transition zone contains the molecular machinery for sorting and controlling the molecular import and export, known as ciliary gating (García-Gonzalo and Reiter, 2017; Park and Leroux, 2022; Wang et al., 2022). In addition, molecules at the ciliary base can regulate ciliary signaling, as recently shown for Shh signaling, which is positively regulated by Numb, a molecule associated with the endocytosis machinery at the ciliary pocket (Liu et al., 2024). Due to its localization ADGRV1 may participate in both, ciliary gating and the regulation of ciliary signaling. Interestingly, the latter function of ADGRV1 would be in line with the previously found association of ADGRV1 with endocytosis in the ciliary pocket (Bauß et al., 2014;

Knapp et al., 2017) and the aforementioned link to the Shh signaling pathway.

Like other aGPCRs, ADGRV1 acts as a metabotropic mechanoreceptor sensing shear stress (Langenhan, 2020; Kusuluri et al., 2021). It is possible, that ADGRV1 is also activated by mechanical shear forces generated at the ciliary base and/or in the ciliary pocket by the bending of the ciliary shaft relative to the cell body. Consequently, the downstream signaling of activated ADGRV1 may regulate the functions described above.

At the base of primary cilia, ADGRV1 physically interacts with the components of the TRiC/CCT chaperonin complex and the three Bardet-Biedel syndrome (BBS) chaperonin-like proteins BBS6, BBS10 and BBS12 (Knapp et al., 2022; Linnert et al., 2023b). Here, we demonstrate that ADGRV1 also functionally interacts with these chaperonins in primary cilia. siRNA-mediated knockdowns of ADGRV1 and CCT2 molecules in hTERT-RPE1 cells lead to a consistent ciliary phenotype, namely altered ciliogenesis paired with reduced ciliary length, as previously reported for BBS chaperonin-like proteins (Hernandez-Hernandez et al., 2013; Patnaik et al., 2019; Hey et al., 2021) indicating that ADGRV1 and the TRiC/CCT-BBS chaperonins are enrolled in overlapping ciliary pathways. Furthermore, we show that the ciliary localization of ADGRV1 at the ciliary base depends on the presence of the chaperonin proteins BBS6, CCT2 and CCT3. ADGRV1 protein is depleted from the ciliary base of primary cilia in cultured cells and from the photoreceptor cilium in retinal tissue sections upon loss of these components. These findings were confirmed by determining the amount of ADGRV1 in protein lysates of BBS6 knockdown cells. However, the absence of BBS6 does not lead to a reduction in transcriptional activity of the *ADGRV1* gene; in fact, *ADGRV1/Adgrv1* mRNA levels were several-fold higher after knockdown *BBS6* or knockout of *Bbs6* in cells and retinal tissue, respectively. The upregulation of *ADGRV1* transcription could be part of a compensatory mechanism that responds to the reduced amount of ciliary ADGRV1 protein. There is evidence that BBS6 regulates the nuclear import of SMARCC1, a chromatin remodeler that modifies gene activity in the developing heart (Scott et al., 2017). However, whether a function of BBS6 in cytoplasmic-nuclear shuttling also plays a role in the transcriptional regulation of *ADGRV1* gene activity needs to be clarified in future studies. In any case, treatments with the proteasomal inhibitor MG123 restore protein expression, demonstrating that the ADGRV1 protein is degraded by the proteasome in the absence of chaperonins.

Substrates for the CCT chaperonin complex are predominantly cytoplasmic proteins such as the cytoskeletal components actin and tubulin as well as several proteins with β -propellers/WD40 repeats (Yam et al., 2008; Vallin and Grantham, 2019). At the base of primary cilia, the CCT chaperonins and BBS chaperonin-like proteins form a CCT/BBS chaperonin complex which associates with a subset of BBS molecules to mediate the assembly of the BBSome (Seo et al., 2010; Zhang et al., 2012; Wingfield et al., 2018). Screens in yeast also demonstrated membrane proteins as putative substrates of CCT chaperonins (Dekker et al., 2008) which is in line with our finding that transmembrane receptor ADGRV1 is a substrate of the CCT/BBS chaperonin complex. We hypothesize that the function of the CCT/BBS chaperonin complex ensures correct ADGRV1 conformation for proper integration of the receptor at the ciliary base. If this is not the case, misfolded

ADGRV1 molecules are transferred to the proteasome for proteolytical degradation. This proteostasis pathway is well known from the ER, where misfolded GPCRs are targeted to the proteasome (Meusser et al., 2005). We have recently shown in patient-derived cells that USH2C defects in ADGRV1 also lead to an increase in autophagy, another important degradation pathway of the cell (Linnert et al., 2023a). Defects in the CCT/BBS chaperonin system can lead to an overload of proteasomal degradation machinery. Previous studies indicated that the absence or dysfunction of the TriC/CCT system leads to an increased load on the two main degradation pathways autophagy and ubiquitin-proteasome system (UPS) (Lobanova et al., 2013; Pavel et al., 2016; Álvarez-Satta et al., 2017). There is evidence that prolonged periods of degradation pathway overload are likely to affect protein homeostasis unbalancing proteostasis associated with inherited retinal degenerations (Lobanova et al., 2013) which possibly is also the case in ADGRV1-related diseases.

Mutations in the genes for *ADGRV1*, *MKKS/BBS6* and *CCT2* are causative for severe syndromic retinopathies, namely USH2C, BBS, and MKKS (Sheffield, 2010; Slavotinek, 2020; Fuster-García et al., 2021) or non-syndromic retinal dystrophies such as Leber congenital amaurosis (LCA) (Minegishi et al., 2016; Weibrecht et al., 2017). Interestingly, in our omics data on interacting proteins of ADGRV1 and DEGs in ADGRV1-deficient systems, we find additional links to molecules associated with further retinal ciliopathy: defects in *CEP250* (atypical USH), *FAM164a* (RP28) or *USH1C*, *PCDH15* (USH1F), *WHRN* (USH2D) (Ahmed et al., 2001; Karlstetter et al., 2014; Khateb et al., 2014; Sorusch et al., 2017; Grotz et al., 2022) all lead to photoreceptor cilia dysfunctions and retinal degenerations in humans and mice. It is therefore plausible that the pathomechanisms leading to retinopathies overlap having a common origin at the photoreceptor cilium. Our findings also raise the possibility of a common treatment target for these diseases, namely, photoreceptor proteostasis. In animal models for autosomal dominant Retinitis pigmentosa due to mutations in the *RHO* gene, recent preclinical findings indicate that treating imbalanced proteostasis by pharmacological inhibition of the VCP/proteasome rescues photoreceptor degeneration (Sen et al., 2021). These findings suggest treatment strategies for some forms of USH, BBS, RP and LCA.

Our findings align with the broader hypothesis that defects in primary cilia structure or signaling contribute to neurological conditions such as epilepsy (Karalis et al., 2022). Mutations in human *CILK1* (ciliogenesis-associated kinase 1) have been linked to both ciliopathies and epilepsy (Limerick et al., 2024) which is consistent with the disease manifestation resulting from mutations in *ADGRV1*. As in the case of pathogenic *ADGRV1* mutations the ciliation rate, the ciliary length, and Shh signaling are altered by *CILK1* mutations. Although there is growing evidence that dysfunctions of primary cilia are associated with epilepsy (Karalis et al., 2022; Vien et al., 2023; Limerick et al., 2024), it is not clear to what extent these are caused by defects in ADGRV1. Whether the dysregulation of glutamate homeostasis in hippocampal astrocytes of the brain of ADGRV1-deficient mice epilepsy (Güler et al., 2024) is associated with cilia defects needs to be determined in future studies.

However, it remains unclear whether the epileptic phenotypes observed in ADGRV1-deficient models are primarily due to ciliary dysfunction or if secondary effects, such as altered glutamate homeostasis, play a more prominent role.

Conclusion

Present data indicate that the aGPCR ADGRV1 is part of the ciliary protein interactome and participants in ciliary signalling pathways. At the ciliary base ADGRV1 interacts with the TriC/CCT-BBS chaperonin co-complex which ensures its correct ciliary localization. Failure of the chaperonin complex leads to proteasomal degradation of ADGRV1 which may result in imbalanced proteostasis in photoreceptor cells. Dysfunction or absence of ADGRV1 from primary cilia may underlay the pathophysiology of human USH type 2 and epilepsy caused by mutations in *ADGRV1*.

Materials and methods

Animals and tissues

Animals were used in accordance with the guidelines set by the Association for Research in Vision and Ophthalmology. The use of mice for research purposes was approved by the local authority, Mainz-Bingen district administration under file number 41a/177-5865-§11 ZVTE on April 30, 2014.

Laboratory mice were housed under 12/12-h light/dark cycles, food and water *ad libitum*. Following mouse models were: *Adgrv1/del7TM* mice express only a truncated form of the *Adgrv1* protein lacking the entire 7-transmembrane and intracellular domain, due to the replacement of 101 bp in exon 82 with a vector containing premature termination codon (McMillan and White, 2004). *Adgrv1/DrumB* mice carry a nonsense mutation (c.8554+2t > c) in intron 37-38 of *Adgrv1*, leading to a premature termination codon (Potter et al., 2016). *Mkks/Bbs6^{-/-}* knockout mice have been previously described by Ross et al. (2005). Breeding background of the mice was the C57BL/6 strain.

Brain tissue, eyeballs and isolated retinae were removed from the sacrificed animals for subsequent experimental protocols. Eyeballs and retinal tissue from *Bbs10^{-/-}* and *Bbs12^{-/-}* complete knockout mice (Cognard et al., 2015) were received from Dr. Vincent Marion (Institut national de la santé et de la recherche médicale, Strasbourg, France).

Antibodies

Following primary antibodies were used: mouse anti-GT335 (AdipoGen, AG-20B-0020), rabbit anti-ARL13B (Proteintech, 17711-1-AP), mouse anti-ARL13B (Proteintech, 66739-1-Ig), mouse anti-CETN3 (Giessler et al., 2004), rabbit anti-CETN3 (Giessler et al., 2004), rabbit anti-ADGRV1 (Reiners et al., 2005), goat anti-CETN2 (Giessler et al., 2004), rabbit anti-BBS6 (Proteintech, 13078-1-AP), mouse anti-GAPDH (Abcam, ab9484), mouse anti-CCT3 (Proteintech, 60264-1-Ig), goat anti-PCTN2 (Santa Cruz Biotechnology, sc-28145). Secondary antibodies were conjugated to Alexa 488, Alexa 555, Alexa 568, Alexa 680, or IR Dye 800, all purchased from Invitrogen or Rockland Immunochemicals. Nuclear DNA was counterstained with DAPI (40,6-diamidino-2-phenylindole, 1 mg/mL, diluted 1:12,000; Sigma-Aldrich).

Cell culture

hTERT-RPE-1 cells: hTERT-immortalized retinal pigment epithelial cells (RPE) were cultured in Dulbecco's Modified Eagle Medium/Nutrient Mixture F-12 (DMEM/F-12) (Thermo Fisher Scientific).

HEK293T cells: Human HEK293T cells were cultivated in Dulbecco's Modified Eagle Medium (DMEM) (Thermo Fisher Scientific) containing 10% heat-inactivated foetal calf serum (FCS). For transient transfections, GeneJuice[®] (Merck Millipore) or Lipofectamine LTX with Plus reagent (Thermo Fisher Scientific) were used according to the manufacturer's instructions.

Human primary fibroblasts: Healthy primary fibroblast lines were expanded from skin biopsies collected from human donors (ethics vote: Landesärztekammer Rhineland-Palatinate to Kerstin-Nagel Wolfrum). ADGRV1 R2959* patient-derived fibroblasts were a kind gift from Dr. Erwin van Wijk (Radboud University Medical Center, Nijmegen) and were derived from skin biopsies of a 57-year-old male USH2C patient who carries a nonsense mutation in the VLGR1/ADGRV1 gene (g. [90006848C>T]) (Usher syndrome database, <https://databases.lovd.nl/shared/variants/GPR98/unique>). The primary human dermal fibroblast lines were *mycoplasma* negative and cultured in DMEM, containing 10% FCS and 1% penicillin-streptomycin at 37°C and 5% CO₂.

To induce growth of primary cilia, cells were cultured for 48 h in serum-free OptiMEM (Thermo Fisher Scientific).

Proteasome inhibition

For the analysis of the proteasome activity in BBS6/CCT2/CCT3 depleted hTERT-RPE1 cells, the proteasome was inhibited by a treatment with MG132 (Sigma). For ciliation experiments, cells were seeded on glass coverslips (15,000 cells). The following day the complete growth media was substituted with serum-free OptiMEM (Thermo Fisher Scientific). To induce growth of primary cilia, cells were starved for 48 h. 5 μM MG132 was added to the cells in the last 2 h. Control cells were treated with an appropriate volume of DMSO.

siRNA-mediated knockdown

hTERT-RPE1 cells were transfected with siRNAs using Lipofectamine RNAiMAX (Invitrogen, Thermo Fisher Scientific) according to the manufacturer's instructions. siRNAs were used for following human genes: *BBS6* (L-013300-00-0005, Dharmacon), *CCT3* (hs.Ri.CCT3.13.1, IDT), *CCT2* (hs.Ri.CCT2.13.1, IDT).

Isolation and culturing of primary murine astrocytes

Hippocampal astrocytes were isolated from newborn mouse pups on postnatal day 0 (PNO) as previously described (Güler et al., 2021). Astrocyte cultures of *Adgrv/del7TM*, *Adgrv1/DrumB^{-/-}* and C57BL/6 were cultivated in DMEM, containing 10% FCS and 1% penicillin-streptomycin at 37°C and 5% CO₂.

Immunocytochemistry of primary cilia

For immunostaining, cells were cultured in 24-well plates on coverslips. Cells were fixed in PBS containing 4% paraformaldehyde for 10 min at room temperature (RT). After fixation cells were washed three times with PBS and permeabilised by using PBST (0.2% Triton-X-100, Roth) for 10 min at RT, washed once with PBS, and incubated for 1 h in blocking solution blocked (0.1% ovalbumin, 0.5% fish gelatine in PBS) at RT. Primary antibodies in blocking solution were incubated overnight at 4°C. Subsequently, cells were washed three times with PBS prior to the incubation with secondary antibodies, containing DAPI, for 1 h at RT. After three washes with PBS, cells were mounted with Mowiol (Roth) prior to microscopic analyses.

Immunohistochemistry

Dissected eye cups were cryofixation in melting isopentane (-168°C) as previously described (Wolfrum, 1991). Cryofixed specimens were cryosectioned in a MICROM HM 560 cryostat (Thermo Scientific). 10–12 μm thick cryosections were placed on 0.01% poly-L-lysine-coated coverslips and encircled by hydrophobic barrier pap pen (Science Services). Subsequently, cryosections were incubated subsequently with 0.01% Tween 20 for permeabilisation, washed several times, and incubated for 45 min in blocking solution at RT. Primary antibodies were incubated overnight at 4°C and after washing, secondary antibodies including DAPI (1 mg/mL, Sigma) were incubated for 1 h at RT. After several washes, sections were mounted in Mowiol (Roth) and stored at 4°C in the dark.

Western blot analysis

Western blotting was performed as previously described (Krzyszko et al., 2022). In brief, protein lysates from cells and tissue were prepared using Triton-X-100 lysis buffer (50 mM Tris/HCl, 150 mM NaCl, 0.5% Triton-X-100, pH 7.4) containing complete protease inhibitor cocktail (Sigma) prior to sonication. Protein content was determined by performing a BCA protein assay (Merck Millipore). SDS-PAGE was performed on a Mini-PROTEAN System (BioRad) and separated proteins were transferred to a polyvinylidene difluoride (PVDF) membrane (Merck Millipore) using the Mini Trans-Blot Electrophoretic Transfer Cell (BioRad). Blot membranes were blocked in AppliChem blocking reagent for 1 h at RT. Primary antibodies were diluted in blocking solution and incubated overnight at 4°C prior to the incubation of secondary antibodies, diluted in blocking solution, for 1 h at RT. Blot membranes were scanned with the Odyssey infrared imaging system (LI-COR Biosciences).

Microscopy, image analysis, and data processing

Mounted cells and tissue were analysed on a Leica DM6000B microscope and digital images were obtained by using a Leica K5 digital camera (Leica) and stored as LIF-files (Software Leica Application Suite). Microscopic images were processed using the Fiji/ImageJ software (Schindelin et al., 2012). For the measurement

of primary cilia length, images were loaded into Fiji using the Bio-Formats plugin. Primary cilia were identified by the markers for the ciliary axoneme and the basal body.

Following previous studies, the ciliary length was measured by applying the Fiji line draw tool. The percentage of ciliated cells, the mean cilia length, and the cumulative distribution of the ciliary length was calculated using R studio (Asante et al., 2014; Bergen et al., 2017; Kilander et al., 2018).

Quantification of anti-ADGRV1 signal at the primary cilia base was measured and calculated by the total corrected cellular fluorescence (TCCF = integrated density- (area of selected cell x mean fluorescence of background readings) (McCloy et al., 2014). The cilia base area was determined by a counterstaining with the ciliary base marker anti-PCTN2. The PCTN2 positive area was then used to measure the anti-ADGRV1 signal.

For densitometry analysis of Western blots, the LI-COR software Image Studio was used. For quantification, we normalised the detected bands to the bands of the housekeeping protein GAPDH.

Statistical analysis and figure preparation was conducted with RStudio (R Core Team, 2022). Cohen's d effect sizes of ciliary measurements were calculated using the psychometrica online tool (Cohen, 2013; Lenhard and Lenhard, 2022).

Reverse transcriptase (RT)-qPCR

Total RNA was isolated from hTERT-RPE1 cells and mouse retinae according to the instructions of the Qiagen RNeasy Mini Kit. RNA quality was determined by a Nanodrop (Thermo Fisher Scientific). RNA was transcribed to cDNA according to the instructions of the SuperScript™ III First-Strand Synthesis SuperMix (Thermo Fisher Scientific). Subsequently, qPCR was performed using a QuantStudio 1 qPCR machine (Thermo Fisher Scientific) and the iTaq Universal SYBR Green Supermix (Bio Rad). Following primers were used: Human: *CCT2* fwd 5'TAAGGCAGGAGCTGATGAAG 3'; rev 5'TTTAGCTGCTGGATTGTCAAC 3'; *CCT3* fwd 5'ATTGTGCTGCTGGATTCTTCTCTG 3'; rev 5'CTGCGGATGGCTGTGATATTGG 3'; *BBS6* fwd 5'AATGACACTGCC TGGGATG 3'; rev 5'TCGTTGTGAGTCTTGTGTCTG 3'; *GAPDH* fwd 5'GAGTCAAGGGATTGGTCGT 3'; rev 5'TTGATTTTGAGGGATCTCG 3'. Mouse: *Gapdh* fwd 5'CGACTTCAACAGCAACTCCACTCTTCC 3'; rev 5'TGGGTGGTCCAGGGTTTCTTACTCCTT 3'; *Bbs6* fwd 5'GTCTGCTCTGCAAGATTGG 3'; rev 5'AAGACGTGCATTGCTGTTGG 3'; *Adgrv1* fwd 5'CCGATGGTGCCAGATATAAAGTAG 3'; rev 5'TCTTCGCTTCCTGGAGAATTG 3'

Analysis of TAP and RNAseq data

With the datasets, differential gene expression analysis and GO enrichment analysis were performed (<https://en.novogene.com/services/research-services/transcriptome-sequencing/mrna-sequencing/>). Databases for GO term analysis and STRING networks of RNAseq data were accessed on 12.06.2024. STRING database for the TAP data was accessed on 13.03.2024.

Data availability statement

Publicly available datasets were analyzed in this study. This data can be found here: The mass spectrometry proteomics data have been deposited to the ProteomeXchange Consortium via the PRIDE partner repository with the dataset identifier PXD042629. The RNA-seq data presented in this study has been deposited in the NCBI Sequence Read Archive (SRA). It is accessible under the BioProject accession numbers: PRJNA1180279 (Adgrv1/del7TM retinae, WT retinae) and PRJNA1180475 (USH2C patient-derived fibroblasts, healthy donor fibroblasts).

Ethics statement

The studies involving humans were approved by Ethics vote: Landesärztekammer Rheinland-Palatinate to Kerstin-Nagel Wolfrum. The studies were conducted in accordance with the local legislation and institutional requirements. The participants provided their written informed consent to participate in this study. The animal study was approved by The local authority, Mainz-Bingen district administration under file number 41a/177-5865-§11 ZVTE on April 30, 2014. The study was conducted in accordance with the local legislation and institutional requirements.

Author contributions

JL: Conceptualization, Data curation, Formal Analysis, Investigation, Methodology, Software, Validation, Visualization, Writing—original draft, Writing—review and editing. DK: Conceptualization, Data curation, Formal Analysis, Investigation, Methodology, Software, Validation, Visualization, Writing—original draft, Writing—review and editing. BG: Data curation, Investigation, Methodology, Software, Validation, Visualization, Writing—original draft, Writing—review and editing. SP: Investigation, Writing—original draft, Writing—review and editing. HM-S: Funding acquisition, Supervision, Writing—original draft, Writing—review and editing. UW: Conceptualization, Funding acquisition, Project administration, Supervision, Writing—original draft, Writing—review and editing.

Funding

The author(s) declare that financial support was received for the research, authorship, and/or publication of this article. This work was supported by the Deutsche Forschungsgemeinschaft (DFG): FOR 2149 -Elucidation of adhesion-GPCR signaling, project number 246212759 (UW) and in the framework of the DFG SPP2127 - Gene and Cell based therapies to counteract neuroretinal degeneration, project number 399487434 (UW) and 498244102 (HLM-S), The Foundation Fighting Blindness (FFB) PPA-0717-0719-RAD (UW), European Community "SYSCILIA" [FP7/2009/241955] (UW), and inneruniversitäre

Forschungsförderung (“Stufe I”) of the Johannes Gutenberg University Mainz (UW).

Acknowledgments

We thank Ulrike Maas, Yvonne Kerner, and Gabi Stern-Schneider for excellent technical assistance, Kerstin Nagel-Wolfrum for critical discussion of the present data, Vincent Marion for kindly providing tissue from Bbs10^{-/-} and Bbs12^{-/-} mice, and Erwin van Wijk for kindly providing ADGRV1 R2959* patient cells.

Conflict of interest

The authors declare that the research was conducted in the absence of any commercial or financial relationships that could be construed as a potential conflict of interest.

The author(s) declared that they were an editorial board member of Frontiers, at the time of submission. This had no impact on the peer review process and the final decision.

References

- Ahmed, Z. M., Riazuddin, S., Bernstein, S. L., Ahmed, Z., Khan, S., Griffith, A. J., et al. (2001). Mutations of the protocadherin gene PCDH15 cause usher syndrome type 1F. *Am. J. Hum. Genet.* 69, 25–34. doi:10.1086/321277
- Álvarez-Satta, M., Castro-Sánchez, S., and Valverde, D. (2017). Bardet-Biedl syndrome as a chaperonopathy: dissecting the major role of chaperonin-like BBS proteins (BBS6-BBS10-BBS12). *Front. Mol. Biosci.* 4, 55. doi:10.3389/fmolb.2017.00055
- Asante, D., Stevenson, N. L., and Stephens, D. J. (2014). Subunit composition of the human cytoplasmic dynein-2 complex. *J. Cell Sci.* 127, 4774–4787. doi:10.1242/jcs.159038
- Avasthi, P., and Marshall, W. F. (2012). Stages of ciliogenesis and regulation of ciliary length. *Differentiation* 83, S30–S42. doi:10.1016/j.diff.2011.11.015
- Bandah-Rozenfeld, D., Mizrahi-Meissonnier, L., Farhy, C., Obolensky, A., Chowers, I., Pe'er, J., et al. (2010). Homozygosity mapping reveals null mutations in FAM161A as a cause of autosomal-recessive retinitis pigmentosa. *Am. J. Hum. Genet.* 87, 382–391. doi:10.1016/j.ajhg.2010.07.022
- Baufß, K., Knapp, B., Jores, P., Roepman, R., Kremer, H., Wijk, E. V., et al. (2014). Phosphorylation of the Usher syndrome 1G protein SANS controls Magi2-mediated endocytosis. *Hum. Mol. Genet.* 23, 3923–3942. doi:10.1093/hmg/ddu104
- Bergen, D. J. M., Stevenson, N. L., Skinner, R. E. H., Stephens, D. J., and Hammond, C. L. (2017). The Golgi protein giantin is required for normal cilia function in zebrafish. *Biol. Open* 6, 1180–1189. doi:10.1242/bio.025502
- Canterini, S., Dragotto, J., Dardis, A., Zampieri, S., De Stefano, M. E., Mangia, F., et al. (2017). Shortened primary cilium length and dysregulated Sonic hedgehog signaling in Niemann-Pick C1 disease. *Hum. Mol. Genet.* 26, 2277–2289. doi:10.1093/hmg/ddx118
- Chivukula, R. R., Montoro, D. T., Leung, H. M., Yang, J., Shamseldin, H. E., Taylor, M. S., et al. (2020). Author Correction: a human ciliopathy reveals essential functions for NEK10 in airway mucociliary clearance. *Nat. Med.* 26, 244–251. doi:10.1038/s41591-019-0730-x
- Cognard, N., Scerbo, M. J., Obringer, C., Yu, X., Costa, F., Haser, E., et al. (2015). Comparing the Bbs10 complete knockout phenotype with a specific renal epithelial knockout one highlights the link between renal defects and systemic inactivation in mice. *Cilia* 4, 10. doi:10.1186/s13630-015-0019-8
- Cohen, J. (2013). *Statistical power analysis for the behavioral sciences*. London, United Kingdom: Routledge.
- Dekker, C., Stirling, P. C., McCormack, E. A., Filmore, H., Paul, A., Brost, R. L., et al. (2008). The interaction network of the chaperonin CCT. *EMBO J.* 27, 1827–1839. doi:10.1038/emboj.2008.108
- Fuster-García, C., García-Bohórquez, B., Rodríguez-Muñoz, A., Aller, E., Jaijo, T., Millán, J. M., et al. (2021). Usher syndrome: genetics of a human ciliopathy. *Int. J. Mol. Sci.* 22, 6723. doi:10.3390/ijms22136723
- García-Gonzalo, F. R., and Reiter, J. F. (2017). Open sesame: how transition fibers and the transition zone control ciliary composition. *CSH Perspect. Biol.* 9, a028134. doi:10.1101/cshperspect.a028134

Generative AI statement

The authors declare that no Generative AI was used in the creation of this manuscript.

Publisher’s note

All claims expressed in this article are solely those of the authors and do not necessarily represent those of their affiliated organizations, or those of the publisher, the editors and the reviewers. Any product that may be evaluated in this article, or claim that may be made by its manufacturer, is not guaranteed or endorsed by the publisher.

Supplementary material

The Supplementary Material for this article can be found online at: <https://www.frontiersin.org/articles/10.3389/fcell.2025.1520723/full#supplementary-material>

Giessl, A., Pulvermüller, A., Trojan, P., Park, J. H., Choe, H. W., Ernst, O. P., et al. (2004). Differential expression and interaction with the visual G-protein transducin of centrin isoforms in mammalian photoreceptor cells. *J. Biol. Chem.* 279, 51472–51481. doi:10.1074/jbc.M406770200

Grotz, S., Schäfer, J., Wunderlich, K. A., Ellederova, Z., Auch, H., Bähr, A., et al. (2022). Early disruption of photoreceptor cell architecture and loss of vision in a humanized pig model of usher syndromes. *EMBO Mol. Med.* 14, e14817. doi:10.15252/emmm.202114817

Güler, B. E., Krzysko, J., and Wolfrum, U. (2021). Isolation and culturing of primary mouse astrocytes for the analysis of focal adhesion dynamics. *Star. Protoc.* 2, 100954. doi:10.1016/j.xpro.2021.100954

Güler, B. E., Linnert, J., and Wolfrum, U. (2023). Monitoring paxillin in astrocytes reveals the significance of the adhesion G protein coupled receptor VLGR1/ADGRV1 for focal adhesion assembly. *Basic Clin. Pharmacol. Toxicol.* 133, 301–312. doi:10.1111/bcpt.13860

Güler, B. E., Zorin, M., Linnert, J., Nagel-Wolfrum, K., and Wolfrum, U. (2024). The adhesion GPCR ADGRV1 controls glutamate homeostasis in hippocampal astrocytes supporting neuron development: first insights into to pathophysiology of ADGRV1-associated epilepsy. *bioRxiv* 2024 (25), 591120. doi:10.1101/2024.04.25.591120

Hamann, J., Aust, G., Araç, D., Engel, F. B., Formstone, C., Fredriksson, R., et al. (2015). International union of basic and clinical pharmacology. XCIV. adhesion G protein-coupled receptors. *Pharmacol. Rev.* 67, 338–367. doi:10.1124/pr.114.009647

Hernandez-Hernandez, V., Pravin Kumar, P., Diaz-Font, A., May-Simera, H., Jenkins, D., Knight, M., et al. (2013). Bardet-biedl syndrome proteins control the cilia length through regulation of actin polymerization. *Hum. Mol. Genet.* 22, 3858–3868. doi:10.1093/hmg/ddt241

Hey, C. A. B., Larsen, L. J., Tümer, Z., Brøndum-Nielsen, K., Grønskov, K., Hjortshøj, T. D., et al. (2021). BBS proteins affect ciliogenesis and are essential for hedgehog signaling, but not for formation of iPSC-derived RPE-65 expressing RPE-Like cells. *Int. J. Mol. Sci.* 22, 1345. doi:10.3390/ijms22031345

Hilgendorf, K. I., Johnson, C. T., and Jackson, P. K. (2016). The primary cilium as a cellular receiver: organizing ciliary GPCR signaling. *Curr. Opin. Cell Biol.* 39, 84–92. doi:10.1016/j.ccb.2016.02.008

Hilgendorf, K. I., Myers, B. R., and Reiter, J. F. (2024). Emerging mechanistic understanding of cilia function in cellular signalling. *Nat. Rev. Mol. Cell Biol.* 25, 555–573. doi:10.1038/s41580-023-00698-5

Hu, Q. X., Dong, J. H., Du, H. B., Zhang, D. L., Ren, H. Z., Ma, M. L., et al. (2014). Constitutive Gai coupling activity of very large G protein-coupled receptor 1 (VLGR1) and its regulation by PDZD7 protein. *J. Bio Chem.* 289, 24215–24225. doi:10.1074/jbc.M114.549816

Human Protein Atlas (2021). The human protein atlas. Available at: <https://www.proteinatlas.org/> (Accessed September 23, 2024).

- Karalis, V., Donovan, K. E., and Sahin, M. (2022). Primary cilia dysfunction in neurodevelopmental disorders beyond ciliopathies. *J. Dev. Biol.* 10, 54. doi:10.3390/jdb10040054
- Karlstetter, M., Sorusch, N., Caramoy, A., Dannhausen, K., Aslanidis, A., Fauser, S., et al. (2014). Disruption of the retinitis pigmentosa 28 gene *Fam161a* in mice affects photoreceptor ciliary structure and leads to progressive retinal degeneration. *Hum. Mol. Genet.* 23, 5197–5210. doi:10.1093/hmg/ddu242
- Khateb, S., Zelinger, L., Mizrahi-Meissonnier, L., Ayuso, C., Koenekoop, R. K., Laxer, U., et al. (2014). A homozygous nonsense CEP250 mutation combined with a heterozygous nonsense *C2orf71* mutation is associated with atypical Usher syndrome. *J. Med. Genet.* 51, 460–469. doi:10.1136/jmedgenet-2014-102287
- Kilander, M. B. C., Wang, C. H., Chang, C. H., Nestor, J. E., Herold, K., Tsai, J. W., et al. (2018). A rare human CEP290 variant disrupts the molecular integrity of the primary cilium and impairs Sonic Hedgehog machinery. *Sci. Rep.* 8, 17335. doi:10.1038/s41598-018-35614-x
- Knapp, B., Kusururi, D. K., Horn, N., Boldt, K., Ueffing, M., and Wolfrum, U. (2017). Identification of protein complexes associated with the usher syndrome 2C and epilepsy-associated protein VLGR1 applying affinity proteomics. *Genom. Comput. Biol.* 4, 100051. doi:10.18547/gcb.2018.vol4.iss1.e100051
- Knapp, B., Roedig, J., Roedig, H., Krzysko, J., Horn, N., Güler, B. E., et al. (2022). Affinity proteomics identifies interaction partners and defines novel insights into the function of the adhesion GPCR VLGR1/ADGRV1. *Molecules* 27, 3108. doi:10.3390/molecules27103108
- Krzysko, J., Maciag, F., Mertens, A., Güler, B. E., Linnert, J., Boldt, K., et al. (2022). The adhesion GPCR VLGR1/ADGRV1 regulates the Ca²⁺ homeostasis at mitochondria-associated ER membranes. *Cells* 11, 2790. doi:10.3390/cells11182790
- Kusururi, D. K., Güler, B. E., Knapp, B., Horn, N., Boldt, K., Ueffing, M., et al. (2021). Adhesion G protein-coupled receptor VLGR1/ADGRV1 regulates cell spreading and migration by mechanosensing at focal adhesions. *iScience* 24, 102283. doi:10.1016/j.isci.2021.102283
- Langenhan, T. (2020). Adhesion G protein-coupled receptors—candidate metabotropic mechanosensors and novel drug targets. *Basic Clin. Pharmacol. Toxicol.* 126, 5–16. doi:10.1111/bcpt.13223
- Langmann, T., Di Gioia, S. A., Rau, I., Stöhr, H., Maksimovic, N. S., Corbo, J. C., et al. (2010). Nonsense mutations in *FAM161A* cause RP28-associated recessive retinitis pigmentosa. *Am. J. Hum. Genet.* 87, 376–381. doi:10.1016/j.ajhg.2010.07.018
- Lee, K. H. (2020). Involvement of Wnt signaling in primary cilia assembly and disassembly. *FEBS J.* 287, 5027–5038. doi:10.1111/febs.15579
- Leng, X., Zhang, T., Guan, Y., and Tang, M. (2022). Genotype and phenotype analysis of epilepsy caused by ADGRV1 mutations in Chinese children. *Seizure* 103, 108–114. doi:10.1016/j.seizure.2022.11.005
- Lenhard, W., and Lenhard, A. (2022). *Computation of effect sizes*. Psychometrica. Available at: https://www.psychometrica.de/effect_size.html (Accessed December 19, 2024).
- Liebscher, I., Schöneberg, T., and Thor, D. (2022). Stachel-mediated activation of adhesion G protein-coupled receptors: insights from cryo-EM studies. *Signal Transduct. Target Ther.* 7, 227. doi:10.1038/s41392-022-01083-y
- Limerick, A., McCabe, E. A., Turner, J. S., Kuang, K. W., Brautigan, D. L., Hao, Y., et al. (2024). An epilepsy-associated *CILK1* variant compromises *KATNIP* regulation and impairs primary cilia and hedgehog signaling. *Cells* 13, 1258. doi:10.3390/cells13151258
- Linnert, J., Güler, B. E., Krzysko, J., and Wolfrum, U. (2023a). The adhesion G protein-coupled receptor VLGR1/ADGRV1 controls autophagy. *Basic Clin. Pharmacol. Toxicol.* 133, 313–330. doi:10.1111/bcpt.13869
- Linnert, J., Knapp, B., Güler, B. E., Boldt, K., Ueffing, M., and Wolfrum, U. (2023b). Usher syndrome proteins ADGRV1 (*USH2C*) and *CIB2* (*USH1J*) interact and share a common interactome containing *TRiC/CCT-BBS* chaperonins. *Front. Cell Dev. Biol.* 11, 1199069. doi:10.3389/fcell.2023.1199069
- Liu, J. Y. W., Dzurova, N., Al-Kaaby, B., Mills, K., Sisodiya, S. M., and Thom, M. (2020). Granule cell dispersion in human temporal lobe epilepsy: proteomics investigation of neurodevelopmental migratory pathways. *Front. Cell Neurosci.* 14, 53. doi:10.3389/fncel.2020.00053
- Liu, Q., Tan, G., Levenkova, N., Li, T., Pugh, E. N., Rux, J. J., et al. (2007). The proteome of the mouse photoreceptor sensory cilium complex. *Mol. Cell Proteomics* 6, 1299–1317. doi:10.1074/mcp.M700054-MCP200
- Liu, X., Vansant, G., Udovichenko, I. P., Wolfrum, U., and Williams, D. S. (1997). Myosin VIIa, the product of the Usher 1B syndrome gene, is concentrated in the connecting cilia of photoreceptor cells. *Cell Motil. Cytoskelet.* 37, 240–252. doi:10.1002/(SICI)1097-0169(1997)37:3<240::AID-CM6>3.0.CO;2-A
- Liu, X., Yam, P. T., Schlienger, S., Cai, E., Zhang, J., Chen, W. J., et al. (2024). Numb positively regulates Hedgehog signaling at the ciliary pocket. *Nat. Commun.* 15, 3365. doi:10.1038/s41467-024-47244-1
- Lobanova, E. S., Finkelstein, S., Skiba, N. P., and Arshavsky, V. Y. (2013). Proteasome overload is a common stress factor in multiple forms of inherited retinal degeneration. *Proc. Natl. Acad. Sci. U. S. A.* 110, 9986–9991. doi:10.1073/pnas.1305521110
- Maerker, T., van Wijk, E., Overlack, N., Kersten, F. F. J., Mcgee, J., Goldmann, T., et al. (2008). A novel Usher protein network at the periciliary reloading point between molecular transport machineries in vertebrate photoreceptor cells. *Hum. Mol. Genet.* 17, 71–86. doi:10.1093/hmg/ddm285
- May-Simera, H., Nagel-Wolfrum, K., and Wolfrum, U. (2017). Cilia - the sensory antennae in the eye. *Prog. Retin Eye Res.* 60, 144–180. doi:10.1016/j.preteyeres.2017.05.001
- McCloy, R. A., Rogers, S., Caldron, C. E., Lorca, T., Castro, A., and Burgess, A. (2014). Partial inhibition of Cdk1 in G2 phase overrides the SAC and decouples mitotic events. *Cell Cycle* 13, 1400–1412. doi:10.4161/cc.28401
- McGee, J. A., Goodyear, R. J., McMillan, D. R., Stauffer, E. A., Holt, J. R., Locke, K. G., et al. (2006). The very large G-protein-coupled receptor VLGR1: a component of the ankle link complex required for the normal development of auditory hair bundles. *J. Neurosci.* 26, 6543–6553. doi:10.1523/JNEUROSCI.0693-06.2006
- McMillan, D. R., Kayes-Wandover, K. M., Richardson, J. A., and White, P. C. (2002). Very large G protein-coupled receptor-1, the largest known cell surface protein, is highly expressed in the developing central nervous system. *J. Bio Chem.* 277, 785–792. doi:10.1074/jbc.M108929200
- McMillan, D. R., and White, P. C. (2004). Loss of the transmembrane and cytoplasmic domains of the very large G-protein-coupled receptor-1 (VLGR1 or Mass1) causes audiogenic seizures in mice. *Mol. Cell Neurosci.* 26, 322–329. doi:10.1016/j.mcn.2004.02.005
- McMillan, D. R., and White, P. C. (2010). Studies on the very large G protein-coupled receptor: from initial discovery to determining its role in sensorineural deafness in higher animals. *Adv. Exp. Med. Biol.* 706, 76–86. doi:10.1007/978-1-4419-7913-1_6
- Meusser, B., Hirsch, C., Jarosch, E., and Sommer, T. (2005). ERAD: the long road to destruction. *Nat. Cell Biol.* 7, 766–772. doi:10.1038/ncb0805-766
- Michalski, N., Michel, V., Bahloul, A., Lefèvre, G., Barral, J., Yagi, H., et al. (2007). Molecular characterization of the ankle-link complex in cochlear hair cells and its role in the hair bundle functioning. *J. Neurosci.* 27, 6478–6488. doi:10.1523/JNEUROSCI.0342-07.2007
- Mill, P., Christensen, S. T., and Pedersen, L. B. (2023). Primary cilia as dynamic and diverse signalling hubs in development and disease. *Nat. Rev. Genet.* 24, 421–441. doi:10.1038/s41576-023-00587-9
- Minegishi, Y., Sheng, X., Yoshitake, K., Sergeev, Y., Iejima, D., Shibagaki, Y., et al. (2016). CCT2 mutations evoke Leber congenital amaurosis due to chaperone complex instability. *Sci. Rep.* 6, 33742. doi:10.1038/srep33742
- Mukherjee, M., Ratnayake, I., Janga, M., Fogarty, E., Scheidt, S., Grassmeyer, J., et al. (2020). Notch signaling regulates Akap12 expression and primary cilia length during renal tubule morphogenesis. *FASEB J.* 34, 9512–9530. doi:10.1096/fj.201902358RR
- Myers, K. A., Nasioulas, S., Boys, A., McMahon, J. M., Slater, H., Lockhart, P., et al. (2018). ADGRV1 is implicated in myoclonic epilepsy. *Epilepsia* 59, 381–388. doi:10.1111/epi.13980
- Novas, R., Cardenas-Rodriguez, M., Lepanto, P., Fabregat, M., Rodao, M., Fariello, M. I., et al. (2018). Kinesin 1 regulates cilia length through an interaction with the Bardet-Biedl syndrome related protein CCDC28B. *Sci. Rep.* 8, 3019. doi:10.1038/s41598-018-21329-6
- Park, K., and Leroux, M. R. (2022). Composition, organization and mechanisms of the transition zone, a gate for the cilium. *EMBO Rep.* 23, e55420. doi:10.15252/embr.202255420
- Patnaik, S. R., Kretschmer, V., Brücker, L., Schneider, S., Volz, A. K., Oancea-Castillo, R. L., et al. (2019). Bardet-Biedl Syndrome proteins regulate cilia disassembly during tissue maturation. *Cell Mol. Life Sci.* 76, 757–775. doi:10.1007/s00018-018-2966-x
- Pavel, M., Imarisio, S., Menzies, F. M., Jimenez-Sanchez, M., Siddiqi, F. H., Wu, X., et al. (2016). CCT complex restricts neuropathogenic protein aggregation via autophagy. *Nat. Commun.* 7, 13821. doi:10.1038/ncomms13821
- Potter, P. K., Bowl, M. R., Jeyarajan, P., Wisby, L., Bleas, A., Goldsworthy, M. E., et al. (2016). Novel gene function revealed by mouse mutagenesis screens for models of age-related disease. *Nat. Commun.* 7, 12444. doi:10.1038/ncomms12444
- R Core Team (2022). *R: a language and environment for statistical computing*. Vienna: R Foundation for Statistical Computing.
- Reiners, J., Nagel-Wolfrum, K., Jürgens, K., Märker, T., and Wolfrum, U. (2006). Molecular basis of human Usher syndrome: deciphering the meshes of the Usher protein network provides insights into the pathomechanisms of the Usher disease. *Exp. Eye Res.* 83, 97–119. doi:10.1016/j.exer.2005.11.010
- Reiners, J., van Wijk, E., Märker, T., Zimmermann, U., Jürgens, K., te Brinke, H., et al. (2005). Scaffold protein harmonin (*USH1C*) provides molecular links between Usher syndrome type 1 and type 2. *Hum. Mol. Genet.* 14, 3933–3943. doi:10.1093/hmg/ddi417
- Roepman, R., and Wolfrum, U. (2007). “Protein networks and complexes in photoreceptor cilia,” in *Subcellular proteomics* (Springer), 209–236.
- Ross, A. J., May-Simera, H., Eichers, E. R., Kai, M., Hill, J., Jagger, D. J., et al. (2005). Disruption of Bardet-Biedl syndrome ciliary proteins perturbs planar cell polarity in vertebrates. *Nat. Genet.* 37, 1135–1140. doi:10.1038/ng1644

- Satir, P., and Christensen, S. T. (2007). Overview of structure and function of mammalian cilia. *Annu. Rev. Physiol.* 69, 377–400. doi:10.1146/annurev.physiol.69.040705.141236
- Schindelin, J., Arganda-Carreras, I., Frise, E., Kaynig, V., Longair, M., Pietzsch, T., et al. (2012). Fiji: an open-source platform for biological-image analysis. *Nat. Methods* 9, 676–682. doi:10.1038/nmeth.2019
- Scholz, N., Langenhan, T., and Schöneberg, T. (2019). “Revisiting the classification of adhesion GPCRs,” in *Ann NY acad sci* (New York, United States: Blackwell Publishing Inc.), 80–95. doi:10.1111/nyas.14192
- Scott, C. A., Marsden, A. N., Rebagliati, M. R., Zhang, Q., Chamling, X., Searby, C. C., et al. (2017). Nuclear/cytoplasmic transport defects in BBS6 underlie congenital heart disease through perturbation of a chromatin remodeling protein. *PLoS Genet.* 13, e1006936. doi:10.1371/journal.pgen.1006936
- Sen, M., Kutsyr, O., Cao, B., Bolz, S., Arango-Gonzalez, B., and Ueffing, M. (2021). Pharmacological inhibition of the VCP/proteasome Axis rescues photoreceptor degeneration in RHOP23H rat retinal explants. *Biomolecules* 11, 1528. doi:10.3390/biom11101528
- Seo, S., Baye, L. M., Schulz, N. P., Beck, J. S., Zhang, Q., Slusarski, D. C., et al. (2010). BBS6, BBS10, and BBS12 form a complex with CCT/TRiC family chaperonins and mediate BBSome assembly. *Proc. Natl. Acad. Sci. U. S. A.* 107, 1488–1493. doi:10.1073/pnas.0910268107
- Sheffield, V. C. (2010). The blind leading the obese: the molecular pathophysiology of a human obesity syndrome. *Trans. Am. Clin. Climatol. Assoc.* 121, 172–182.
- Shin, D., Lin, S. T., Fu, Y. H., and Ptáček, L. J. (2013). Very large G protein-coupled receptor 1 regulates myelin-associated glycoprotein via Gas/Gaq-mediated protein kinases A/C. *Proc. Natl. Acad. Sci. U. S. A.* 110, 19101–19106. doi:10.1073/pnas.1318501110
- Slavotinek, A. M. (2020). “McKusick-kaufman syndrome,” in *Gene reviews*. Editors M. P. Adam, J. Feldman, G. M. Mirzaa, R. A. Pagon, and S. E. Wallace Seattle WA: University of Washington.
- Sorusch, N., Baub, K., Plutniok, J., Samanta, A., Knapp, B., Nagel-Wolfrum, K., et al. (2017). Characterization of the ternary Usher syndrome SANS/ush2a/whirlin protein complex. *Hum. Mol. Genet.* 26, 1157–1172. doi:10.1093/hmg/ddx027
- Sorusch, N., Yildirim, A., Knapp, B., Janson, J., Fleck, W., Scharf, C., et al. (2019). SANS (USH1G) molecularly links the human usher syndrome protein network to the intraflagellar transport module by direct binding to IFT-B proteins. *Front. Cell Dev. Biol.* 7, 216. doi:10.3389/fcell.2019.00216
- Specht, D., Wu, S. B., Turner, P., Dearden, P., Koentgen, F., Wolfrum, U., et al. (2009). Effects of presynaptic mutations on a postsynaptic Cacna1s calcium channel colocalized with mGluR6 at mouse photoreceptor ribbon synapses. *Invest. Ophthalmol. Vis. Sci.* 50, 505–515. doi:10.1167/iovs.08-2758
- Uhlén, M., Fagerberg, L., Hallström, B. M., Lindskog, C., Oksvold, P., Mardinoglu, A., et al. (2015). Proteomics. Tissue-based map of the human proteome. *Science* 347, 1260419. doi:10.1126/science.1260419
- Vallin, J., and Grantham, J. (2019). The role of the molecular chaperone CCT in protein folding and mediation of cytoskeleton-associated processes: implications for cancer cell biology. *Cell Stress Chaperon* 24, 17–27. doi:10.1007/s12192-018-0949-3
- Van Dam, T. J. P., Kennedy, J., van der Lee, R., de Vrieze, E., Wunderlich, K. A., Rix, S., et al. (2019). Ciliacarta: an integrated and validated compendium of ciliary genes. *PLoS One* 14, e0216705. doi:10.1371/journal.pone.0216705
- van Wijk, E., van der Zwaag, B., Peters, T., Zimmermann, U., te Brinke, H., Kersten, F. J., et al. (2006). The DFNB31 gene product whirlin connects to the Usher protein network in the cochlea and retina by direct association with USH2A and VLGR1. *Hum. Mol. Genet.* 15, 751–765. doi:10.1093/hmg/ddi490
- Vasquez, S. S. V., van Dam, J., and Wheway, G. (2021). An updated SYSCILIA gold standard (SCGSv2) of known ciliary genes, revealing the vast progress that has been made in the cilia research field. *Mol. Biol. Cell* 32, br13. doi:10.1091/mbc.E21-05-0226
- Vien, T. N., Ta, M. C., Kimura, L. F., Onay, T., and DeCaen, P. G. (2023). Primary cilia TRP channel regulates hippocampal excitability. *P Natl. Acad. Sci. U. S. A.* 120, e2219686120. doi:10.1073/pnas.2219686120
- Wang, L., Wen, X., Wang, Z., Lin, Z., Li, C., Zhou, H., et al. (2022). Ciliary transition zone proteins coordinate ciliary protein composition and ectosome shedding. *Nat. Commun.* 13, 3997. doi:10.1038/s41467-022-31751-0
- Wang, Y., Fan, X., Zhang, W., Zhang, C., Wang, J., Jiang, T., et al. (2015). Deficiency of very large G-protein-coupled receptor-1 is a risk factor of tumor-related epilepsy: a whole transcriptome sequencing analysis. *J. Neurooncol* 121, 609–616. doi:10.1007/s11060-014-1674-0
- Weihbrecht, K., Goar, W. A., Pak, T., Garrison, J. E., DeLuca, A. P., Stone, E. M., et al. (2017). Keeping an eye on Bardet-Biedl syndrome: a comprehensive review of the role of Bardet-Biedl syndrome genes in the eye. *Med. Res. Arch.* 5, 1526. doi:10.18103/mra.v5i9.1526
- Weston, M. D., Luijckdijk, M. W. J., Humphrey, K. D., Möller, C., and Kimberling, W. J. (2004). Mutations in the VLGR1 gene implicate G-protein signaling in the pathogenesis of Usher syndrome type II. *Am. J. Hum. Genet.* 74, 357–366. doi:10.1086/381685
- Wolfrum, U. (1991). Centrin- and α -actinin-like immunoreactivity in the ciliary rootlets of insect sensilla. *Cell Tissue Res.* 266, 231–238. doi:10.1007/bf00318178
- Wolfrum, U. (1995). Centrin in the photoreceptor cells of mammalian retinae. *Cell Motil. Cytoskelet.* 32, 55–64. doi:10.1002/cm.970320107
- Yam, A. Y., Xia, Y., Lin, H.-T. J., Burlingame, A., Gerstein, M., and Frydman, J. (2008). Defining the TRiC/CCT interactome links chaperonin function to stabilization of newly made proteins with complex topologies. *Nat. Struct. Mol. Biol.* 15, 1255–1262. doi:10.1038/nsmb.1515
- Yang, J., Liu, X., Zhao, Y., Adamian, M., Pawlyk, B., Sun, X., et al. (2010). Ablation of whirlin long isoform disrupts the USH2 protein complex and causes vision and hearing loss. *PLoS Genet.* 6, e1000955. doi:10.1371/journal.pgen.1000955
- Zhang, Q., Yu, D., Seo, S., Stone, E. M., and Sheffield, V. C. (2012). Intrinsic protein-protein interaction-mediated and chaperonin-assisted sequential assembly of stable bardet-biedl syndrome protein complex, the BBSome. *J. Bio Chem.* 287, 20625–20635. doi:10.1074/jbc.M112.341487
- Zhou, P., Meng, H., Liang, X., Lei, X., Zhang, J., Bian, W., et al. (2022). ADGRV1 variants in febrile seizures/epilepsy with antecedent febrile seizures and their associations with audio-visual abnormalities. *Front. Mol. Neurosci.* 15, 864074. doi:10.3389/fnmol.2022.864074
- Zou, J., Chen, Q., Almishaal, A., Mathur, P. D., Zheng, T., Tian, C., et al. (2017). The roles of USH1 proteins and PDZ domain-containing USH proteins in USH2 complex integrity in cochlear hair cells. *Hum. Mol. Genet.* 26, 624–636. doi:10.1093/hmg/ddw421